

RESEARCH PAPER



Bacillus coagulans ameliorates inflammatory bone loss in post-menopausal osteoporosis via modulating the “Gut-Immune-Bone” axis

Leena Sapra^a, Chaman Saini^a, Pradyumna K. Mishra^b, Bhavuk Garg^c, Sarika Gupta^d, Vikrant Manhas^c, and Rupesh K. Srivastava^a

^aTranslational Immunology, Osteoimmunology & Immunoporosis Lab (TIOIL), An ICMR-Collaborating Centre of Excellence in Bone Health, Department of Biotechnology, All India Institute of Medical Sciences (AIIMS), New Delhi, India; ^bDepartment of Molecular Biology, ICMR-National Institute for Research in Environmental Health, Bhopal, India; ^cDepartment of Orthopaedics, All India Institute of Medical Sciences (AIIMS), New Delhi, India; ^dMolecular Science lab, National Institute of Immunology (NII), New Delhi, India

ABSTRACT



Osteoporosis is a systemic skeletal disease that leads to lower bone mineral density and intensifies the risk of unexpected fractures. Recently, our group reported that numerical defect in the frequencies of Bregs along with their compromised tendency to produce IL-10 cytokine further aggravates inflammatory bone loss in post-menopausal osteoporosis (PMO). Dysbiosis induced mucosal injury and leaky gut are the predominant contributors involved in the progression of inflammatory diseases including PMO. Furthermore, several evidence suggest that gut microbial composition plays a crucial role in the development and differentiation of Bregs. Nevertheless, the potential role of dysbiotic gut microbiota (GM) and Bregs under estrogen deficient PMO conditions has never been deciphered. Here, we evaluated the role of GM in the onset and progression of PMO along with its role in modulating the anti-osteoporotic potential of Bregs. We found that enhancement in the endotoxin producing bacteria and concomitant reduction in the short chain fatty acids producing bacteria, both under pre-clinical and clinical osteoporotic condition augment inflammatory bone loss. This suggests that dysbiosis of GM potentially exacerbates bone deterioration under estrogen deficient PMO conditions. Remarkably, supplementation of probiotic *Bacillus coagulans* significantly improved the bone mineral density, bone strength, and bone micro architecture by modulating the anti-osteoclastogenic, immunosuppressive and immunomodulatory potential of Bregs. The present study delves deeper into the role of immune homeostasis (“Breg-Treg-Th17” cell axis) and GM profile in the pathophysiology of PMO. Altogether, findings of the present study open novel therapeutic avenues, suggesting restoration of GM composition as one of the viable therapeutic options in mitigating inflammatory bone loss under PMO conditions via modulating the “Gut-Immune-Bone” axis.


ARTICLE HISTORY

Received 9 July 2024
Revised 11 March 2025
Accepted 7 April 2025

KEYWORDS

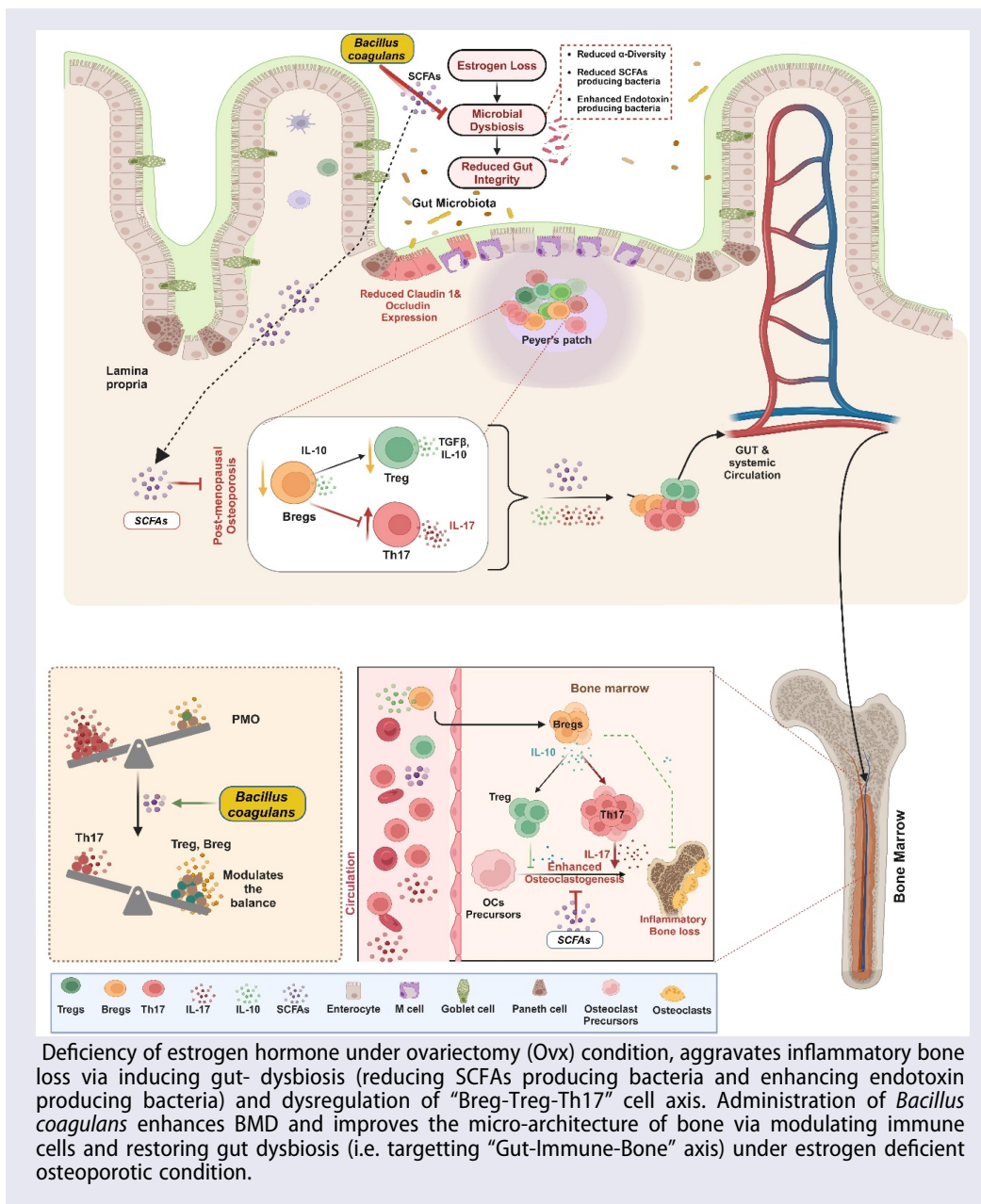
Bacillus coagulans (BC); SCFAs; GUT; regulatory B cells; osteoclast; osteoporosis; immunoporosis and bone health

CONTACT Rupesh K. Srivastava  rupesh_srivastava13@yahoo.co.in; rupeshk@aiims.edu  Translational Immunology, Osteoimmunology & Immunoporosis Lab (TIOIL), An ICMR-Collaborating Centre of Excellence in Bone Health, Department of Biotechnology, All India Institute of Medical Sciences (AIIMS), New Delhi 110029, India

 Supplemental data for this article can be accessed online at <https://doi.org/10.1080/19490976.2025.2492378>

© 2025 The Author(s). Published with license by Taylor & Francis Group, LLC.

This is an Open Access article distributed under the terms of the Creative Commons Attribution-NonCommercial License (<http://creativecommons.org/licenses/by-nc/4.0/>), which permits unrestricted non-commercial use, distribution, and reproduction in any medium, provided the original work is properly cited. The terms on which this article has been published allow the posting of the Accepted Manuscript in a repository by the author(s) or with their consent.



Introduction

Osteoporosis is a systemic skeletal disorder which is characterized by the higher deterioration of the bone tissues and occurrence of lower energy fractures.^{1–4} In 2018, to emphasize the significance of immune system in the pathophysiology of osteoporosis, our group has coined the term “Immunoporosis” (i.e. immunology of osteoporosis).² Recently, our group reported that reduction in the frequencies of Bregs and its tendency to produce IL-10 cytokine is significantly reduced in post-menopausal osteoporosis

(PMO) thus further aggravating inflammatory bone loss.⁵ Several evidences suggest that multiple parameters regulate the development of immune system, and among them Gut-Microbiota (GM) plays a very important role,⁶ as the interplay between the GM and immune system is believed to contribute to the pathogenesis of various immune-mediated diseases including bone pathologies i.e., “Osteomicrobiology”.^{7–9}

In 2014, a study demonstrated that differentiation of Bregs is regulated by the GM¹⁰ and dysbiosis of GM (antibiotic, housing conditions, etc.) reduced the frequencies and functions of Bregs.¹⁰

In addition, the GM derived short chain fatty acid (SCFAs viz. butyrate) via activating aryl hydrocarbon receptor (AhR) supports the functions of Bregs, thereby further suppressing the differentiation of both plasma blast and germinal center (GC) B cells.¹¹ Mounting evidences further suggest that the association between Bregs and microbiota is crucial to limit the pathogenesis of autoimmune diseases along with maintaining tolerance for organ transplantations.^{11,12} Enteric bacteria's activate IL-10 producing B cells (via TLR2, MyD88 and PI3K pathways) and thus maintain mucosal homeostasis.¹³ Altogether these findings reveal the pivotal role of GM in regulating the differentiation and functionality of Bregs. Multiple convincing evidence reported that dysbiosis of GM is interlinked with the pathogenesis of intestinal and extra-intestinal diseases viz. bone diseases (rheumatoid arthritis-RA, osteoarthritis, osteoporosis etc.).¹⁴ Few studies reported that bone loss observed under estrogen deficient PMO conditions is closely linked with the host immunity, which is further influenced by the GM.^{7,8} However, no study delineated whether the observed dysregulated-Bregs in PMO is primarily caused by the dysbiotic GM. Thus, in the present study, we investigate whether restoring the dysbiotic GM under PMO conditions could be a viable strategy in mitigating inflammatory bone loss via modulating the immunoporotic potential of Bregs.

To our knowledge, this is the first study which reveals that deficiency of estrogen hormone leads to dysbiosis induced leaky gut thereby further enhancing the burden of gut inflammation in PMO. Our findings demonstrated that the reduction in the abundance of *Firmicutes* augments inflammatory bone loss in PMO. Importantly, *Firmicutes* are the predominant producers of SCFAs. Thus, in the present study we investigated the bone health modulating potential of lactic acid producing bacteria (LAB) which are primary producers of SCFAs. *Bacillus coagulans* (BC) is a lactic acid producing bacteria that can withstand the lower pH of the stomach and is known to possess immunomodulatory potential. Importantly, US Food and Drug Administration (FDA) has granted BC with Generally Recognized As Safe (GRAS) status. Moreover, genomic analysis of BC revealed that the antibiotics resistance related genes in the species are not transferred to other

bacteria.^{15,16} In addition, a randomized clinical trial demonstrated that BC is safe and effective and can be employed as an adjunct therapy for RA patients.¹⁷ The present study thus unequivocally demonstrated that administration of BC augments the anti-osteoclastogenic, immunosuppressive and immunomodulatory potential of Bregs, via inducing the production of GM derived SCFAs, even under estrogen deficient conditions. Altogether, the present study establishes the nexus between “Gut-Immune-Bone” axis under both pre-clinical and clinical settings and thereby opens novel avenues for employing BC as a probiotic of choice for the treatment and management of inflammatory bone loss observed in PMO.

Material and methods

Reagents and antibodies

Antibodies employed in the study were procured from eBiosciences (USA) and Biolegend (USA): PerCp-Cy5.5-Anti-Mouse-CD4-(550954), PE-Anti-Mouse-B220, PerCp-Cy5.5-Anti-Mouse-CD19-(45-0193-82), BV421-Anti-Mouse-IL-10-(505022), APC-Anti-Mouse-CD1d-(17-0011-82), PECy7-Anti-Mouse-CD5-(25-0051-81), BV785-Anti-Mouse-IL-17-(506928), APC-Anti-Mouse-Foxp3-(17-5773-82) etc. RBC lysis buffer (RBC)-(00-4300-54), Foxp3/Transcription factor staining buffer (0-5523-00) and CellTrace™ carboxyfluorescein succinimidyl ester (CFSE) Cell Proliferation Kit (C34554) were procured from eBiosciences (USA). Acid phosphatase leukocyte (TRAP) kit and short chain fatty acids (acetate, propionate, butyrate) were purchased from Sigma (USA). Macrophage Colony Stimulating Factor (M-CSF-300-25) and Receptor Activator of Nuclear Factor Kappa B (RANKL-310-01), Murine-IL-2-(AF-212-12), Murine-IL-6-(AF-216-16), Human-TGF- β -1-(AF-100-21C), Murine-IL-23-(200-23) were procured from PeproTech (USA). RPMI-1640 and α -minimal essential media were purchased from Gibco (USA). *Bacillus coagulans* (Unique IS-2) was procured from Unique Biotech Ltd., Hyderabad, India. Following ELISA kits were brought from BD (USA): Mouse-TNF- α , Mouse-IL-6, Mouse-IL-17, Mouse-IL-10 and Mouse-IFN γ .

Post-menopausal osteoporotic (PMO) mice model

All *in vitro* and *in vivo* experiments were carried out on 8 to 10 wks old female C57BL/6 mice. Mice were kept in specific pathogenic free (SPF) condition at the animal facility of All India Institute of Medical Sciences (AIIMS), New Delhi, India. For the *in vivo* experiment, mice were randomly allocated into following groups: Sham (healthy control-ovaries intact), Ovariectomized (Ovx-ovaries removed) and Ovx + BC. After one week of post-operative care (POC), Ovx + BC mice were orally gavaged with BC suspension (10^9 cfu) in autoclaved drinking water for 60 days. At the end of experiment, mice from all the groups were euthanized and blood, bones and lymphoid organs were harvested for osteoimmune parameters analysis. All the measures were carried out after the approval of the protocol submitted to the Institutional Animal Ethics Committee of AIIMS (337/IAEC-1/2021), New Delhi, India.

Histological analysis

After fixation, paraffin embedded sections ($5\ \mu\text{m}$) from the large intestine tissues were processed for the histological hematoxylin (H) and eosin (E) analysis and were imaged using microscope.

Intestinal permeability assay

Intestinal permeability in all the respective groups was evaluated via FITC Dextran assay. Briefly, mice were first starved for food and water for 4 h and then orally gavaged with $200\ \mu\text{l}$ of $80\ \text{mg/ml}$ FITC dextran and again deprived of food and water for 4 h. For evaluating the gut integrity, plasma level of FITC dextran was estimated via fluorescence intensity using an excitation wavelength ($488\ \text{nm}$) and an emission wavelength ($528\ \text{nm}$) via using a NanoDrop spectrophotometer/fluorimeter (BioTek Synergy H1).

16S rRNA microbial community analysis

At day 45, fecal pellets from mice groups (sham, Ovx and Ovx + BC) and stool samples from both healthy control ($n = 10$) and PMO ($n = 10$) human subjects were collected via sterile swab in sterile

tube and immediately stored in -80°C for metagenome analysis. Metagenomic DNA was extracted from the mouse and human fecal samples using the commercially available QIAamp DNA stool mini kit (QIAGEN) as per the manufacturer's instructions. Quality of the extracted metagenomic DNA samples were analyzed using NanoDrop via determining A260/280 ratio. QC passed samples were then processed for the first amplicon generation followed by NGS library preparation using Nextera XT Index kit (Illumina Inc.). The QC passed libraries were sequenced on Illumina MiSeq platform. Alpha diversity of samples was determined for all the samples. Number of observed features (ASVs), Simpson index, Simpson reciprocal, Shannon index, Chao1 and Goods coverages were employed as an alpha diversity measures. QIIME2 pipeline was used for microbiome analysis. High quality clean reads were obtained using Trimmomatic v0.38 to remove adapter sequences, ambiguous reads (reads with unknown nucleotides "N" larger than 5%), and low-quality sequences (reads with more than 10% quality threshold (QV) < 25 phred score) along with a sliding window of 20 bp and a minimum length of 100 bp. PE data into single end reads were done using FLASH. High-quality clean reads were then denoised and chimeric sequences were filtered through DADA2. Taxonomic classification of amplicon sequence variants was performed with the q2-feature classified using a pre-trained classifier based on the SILVA database. Diversity metrics of within sample (α -diversity; Shannon's Index) and between samples (β -diversity; weighted and unweighted UniFrac) were calculated. Statistical significance of diversity metrics was also assessed using QIIME2. Shannon's Index observed featured and UniFrac measurements were analyzed with Kruskal–Wallis test and PERMANOVA, respectively.

Quantitative PCR (q-PCR)

According to the manufacturer's instructions, RNA was extracted from the colon tissues using RNeasy Mini Kit (Qiagen, USA). Quality of RNA was estimated via employing Bio Analyzer (Agilent Technologies, Singapore) and samples with RNA Integration Number (RIN) value ≥ 7 were further

processed. Amount of RNA was also quantified using spectrophotometer (Nanodrop Technologies, USA). For cDNA conversion, c-DNA synthesis kit was used (Thermo Scientific, USA). Triplicate samples of cDNA from each group were amplified using customized primers for claudin-1 and occludin normalized with arithmetic mean of GAPDH house-keeping gene. 25 ng of c-DNA was utilized per reaction in each well containing 2X SYBR green PCR master mix (Promega, USA) along the primers. Lastly, threshold cycles values were normalized and expressed as relative gene expression.

Micro-computed tomography (μ -CT) measurements

After dissecting animals, hind limbs were collected, and all the muscles were cleaned from bones. These bone samples were stored in 4% paraformaldehyde. The μ CT scanning was performed at National Institute of Immunology (NII) on Quantum GXII, (Revvity, USA) using the Aluminum 0.5 + copper 0.5 filter with the following parameters: time 14 minutes, Voxel Size 18 micrometer, tube voltage 90 kV, and tube current 180 mA. Sub reconstruction of the acquired image was also performed to generate Sub-volume vox files with a size of 18 μ m. Analyzer 14.0 was used to create 3D reconstructed images of trabecular and cortical bone microarchitecture from serial 2D coronal and axial pictures CT scans (Revvity, USA) by manually selecting the correct region of interest.

Co-culturing of Bregs with bone marrow cells (BMCs) for osteoclastogenesis

As previously mentioned, mouse BMCs were used to generate osteoclasts. BMCs were harvested from the femur and tibiae of 8–10-week-old mice, and RBC lysis was carried out by using 1X RBC lysis buffer. Following RBC lysis, cells were cultured overnight in a T-25 flask using endotoxin-free-MEM media (10% FBS) supplemented with M-CSF (35 ng/ml). Next day, non-adherent cells (BMCs) were collected and co-cultured with Bregs harvested from sham, Ovx, and Ovx + BC mice in a 96 well plate at different cell ratios for 4 days in the presence of M-CSF (30 ng/ml) and RANKL (60

ng/ml). The media was replenished every two days with fresh M-CSF and RANKL factors. The tartrate resistant acid phosphatase (TRAP) staining procedure was carried out after 4 days of incubation.

T cell suppression assay

To investigate the immunosuppressive effect of Bregs in different groups, 2×10^5 Breg cells (harvested from different groups) were co-cultured together with the CFSE labeled CD4⁺CD25⁺ T cells at 1:1 ratio in the presence of anti-CD3 (10 μ g/ml) and CD28 (2 μ g/ml) mAbs at 37°C for 72 h. The proliferation of CD4⁺CD25⁺ T cells was assessed by the quantification of fluorescence intensities of CFSE. The expression of Tregs (CD4⁺Foxp3⁺) and Th17 (CD4⁺IL-17⁺) was evaluated by FACS.

Flow cytometry

For estimating the level of cytokines intracellularly, cells were harvested from distinct lymphoid organs and after processing, cells were resuspended in RPMI-1640 media and seeded at cell density of 1×10^6 cells in 96 well plate. For stimulation, cells were stimulated with phorbol 12-myristate 13-acetate (PMA) (50 ng/ml) and Ionomycin (1 μ g/ml) for 5 h and for last 2.5 h protein transport inhibitor was added. Cells were further harvested and stained with specific cell surface and intracellular marker antibodies labeled with distinct fluorochromes. For evaluating the frequencies of Breg, Treg and Th17 cells, flow cytometry was carried out. For the same, cells were first stained with antibodies specific for cell surface markers such as CD19 for Bregs and CD4 for Tregs and Th17 and incubated for 30–45 min on ice in dark with intermittent gentle tapping every 15 min. After incubation, cells were washed, fixed and permeabilized with 1X fixative/permeabilization buffer and intracellular staining was carried out using BV421-Anti-Mouse-IL-10 and BV785-Anti-Mouse-IL-17 antibodies. After washing, cells were acquired on BD FACSymphony (USA). Data was then analyzed using FlowJo_V10.8.1 (Tree Star, Woodburn, BD USA) software.

Analysis of short chain fatty acids (SCFAs)

SCFAs content in the fecal matter of mice was determined with the help of high-performance liquid chromatography (HPLC). For the same 300 mg of the fecal sample was weighed and 1 ml of Milli Q and 100 μ l of HCl were added to the fecal sample. The fecal sample was then completely homogenized with the help of the vortex (2–3 minutes) and placed for 20 minutes with shaking in between. After 20 minutes sample was centrifuged at 13,850 \times g for 10 minutes at 4°C. Supernatant was collected and transferred to the 2 ml Eppendorf. 600 μ l of diethyl ether was added to the supernatant and continued extraction for 20 minutes. After 20 minutes of extraction, samples were centrifuged at 850 \times g for 5 minutes at 4°C. 400 μ l of the supernatant or organic layer was collected and added to the 500 μ l of the NaOH. Continued extraction for 20 minutes and subsequently centrifuged the sample at 850 \times g for 5 minutes. Discarded the ether layer or organic layer and collected 450 μ l of the aqueous layer or water-soluble layer. Then added water-soluble layer to the 300 μ l of HCl and immediately filtered the sample through the 0.22-micron filter. Next samples were acquired on HPLC machine (LC-20AD, Shimadzu). HPLC conditions used were as follows: Xterra C18 column (250 mm \times 4.6 mm \times 3.5 μ m); mobile phase, 10 mM H₂SO₄ (Isocratic gradient); flow rate, 0.6 mL/min; run time: 11 minutes, wavelength: 210 nm. SCFAs level was determined using the standard calibration curves.

Osteoclasts differentiation from human PBMCs

PBMCs were isolated from the heparinized blood of healthy control (HC) and post-menopausal osteoporotic patients via gently layering the blood on the Histopaque at 1:3 in 15 ml falcon and centrifuged at 800 \times g for 20 min at room temperature (RT) with brake off. After centrifugation, buffy coat was carefully collected and washed twice with 1X PBS via centrifuging the tube at 400 \times g and 300 \times g for 10 min at 4°C. PBMCs were counted and seeded in 96 well plate at cell density 1X 10⁶ cells/well and plate was incubated for 2 h in 5% CO₂ incubator and washed thrice with α -MEM media. Once adhered, cells were incubated with the osteoclastogenic factors RANKL (100 ng/ml) and

M-CSF (30 ng/ml) in the presence or absence of SCFAs (viz. acetate, propionate and butyrate) at different concentrations and the plate was incubated for 14 days in CO₂ incubator. At the end of incubation, TRAP staining was carried out for assessing the generation of multinucleated osteoclasts, counted and imaged using an inverted microscope (EVOS, Thermo Scientific, USA and Image J software, NIH, USA). All the measures were performed after the due approval of the protocols submitted to the Institute Ethics Committee for Post Graduate Research (IECPG-482), AIIMS, New Delhi, India.

Statistical analysis

GraphPad Prism version 9.0 was used for statistical analysis (San Diego, California, USA). Data were represented as mean \pm SEM and $p < 0.05$ value was regarded as statistically significant. Spearman's rank correlation coefficient was carried out for correlation analysis and $p < 0.05$ was considered significant.

Results

Estrogen deficiency leads to loss of gut-barrier integrity and gut-dysbiosis

Dysbiosis-induced “Leaky Gut and mucosal injury” is one of the major contributing factors in the progression of various autoimmune and pathological conditions such as RA, systemic lupus erythematosus (SLE), osteoporosis, etc. We were thus first interested in evaluating the effect of estrogen deficiency on gut-barrier integrity and the diversity of gut-microbial composition. Strikingly, histological analysis demonstrated significant enhancement in the pathological damage to the colonic mucosa in OvX group in comparison to control group (Figure 1(a)). Furthermore, the colon length (indicative of inflamed gut) was also observed to be significantly reduced in the OvX group (Figure 1(b–c)). Of note, we observed that deficiency of estrogen hormone significantly enhanced the leakiness in the gut and disrupts the gut barrier function as evidenced by the enhanced leakage of FITC-Dextran (high fluorescence intensity) in the peripheral circulation of OvX mice (Figure 1(d)). Furthermore, the transcriptional levels of both claudin-1 and occludin (tight junctional proteins) in the intestine were significantly reduced in OvX mice under estrogen

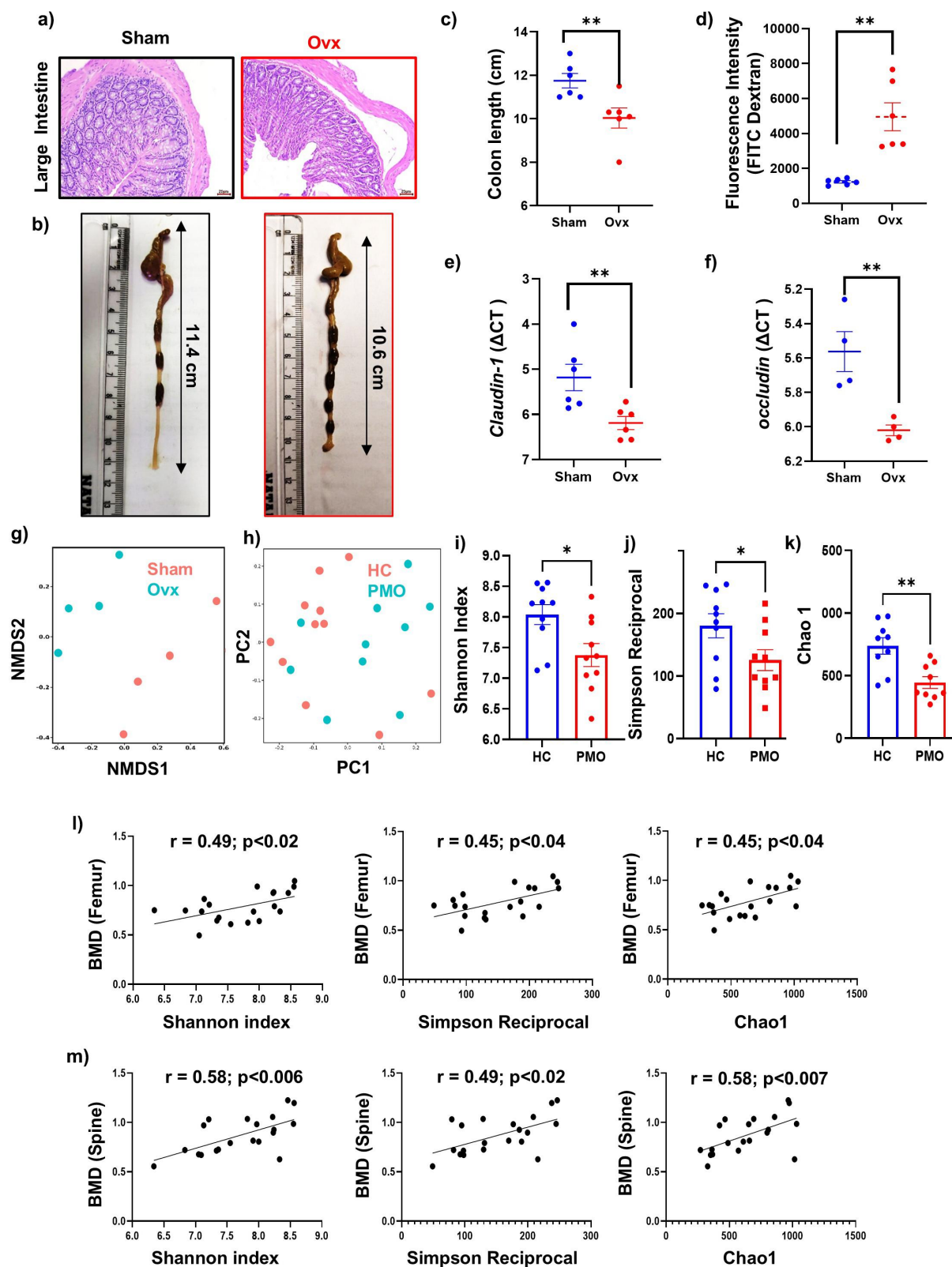


Figure 1. Estrogen deficiency leads to loss of gut-barrier integrity and gut dysbiosis in Ovx mice: (a) H&E staining of large intestine tissues at 20× magnification (20 μm). (b-c) Colon length. (d) Measurement of gut integrity in sham and Ovx operated mice. FITC dextran was administered orally to each experimental mice. Fluorescence intensity was measured at excitation: 488 nm and 528 nm emission as an indicative of gut integrity. (e-f) Relative gene expression of tight junctional proteins claudin-1 and occludin in the large intestine. (g) Nonmetric multidimensional scaling (NMDS) plot representing community composition of bacteria in mice fecal samples. (h) Principal component analysis (PCA) plot showing bacterial communities in human stool samples (healthy control-HC and post-

deficiency (Figure 1(e–f)). These results clearly indicated the pathological role of estrogen deficiency in inducing gut-barrier disruption in PMO mice, thereby further enhancing inflammatory bone loss. Leaky gut is a manifestation of dysbiotic GM composition under various inflammatory conditions. Thus, we further looked into the effect of estrogen deficiency on GM composition. Remarkably, we observed that deficiency of estrogen hormone alters the community composition of bacteria in the stool samples of mice and human subjects (Figure 1(g,h)). Also, we next observed that the alpha diversity (community richness and diversity) of microbial species was significantly reduced in PMO patients in comparison to the HC subjects (Figure 1(i–k)). Intriguingly, we observed that the alpha diversity was positively correlated with the bone mineral density (BMD) for both the femoral and spine regions in human samples (Figure 1(l–m)), thereby strongly suggesting toward the vital role of microbial richness/diversity in maintaining bone health. Moreover, abundance of microbial community analysis represented that Firmicutes, Actinobacteria, Bacteroidetes and Proteobacteria accounted for the predominant phyla in the total diversity (Figure 2(a–b)). The abundance of Firmicutes and Bacteroidetes was further observed to be reduced and increased respectively in the PMO group as compared to the control group (Figure 2(a–b)). Furthermore, alterations were observed at both genus and species levels in the PMO group (Figure 2(c–e)) (Figure S1a–b) (Figure S2a–b). Taken together, these results clearly indicated that deficiency of estrogen hormone augments dysbiosis and reduces gut-integrity thereby further enhancing the burden of gut inflammation observed under postmenopausal osteoporotic conditions.

Bacillus coagulans (BC) maintains bone-microarchitecture in Ovx mice

Above findings indicated reduction in the relative abundance of beneficial lactic acid producing bacteria (LAB) in the PMO group, clearly suggesting that

deficiency of LABs might further augment inflammatory bone loss in PMO mice. Several reports demonstrated that LABs offer distinct advantages and are potential probiotics that inhibits the growth of harmful organisms, improve nutrients absorption along with maintaining immune homeostasis.¹⁸ Thus, we next proposed to administer BC (LAB) in our pre-clinical mice model for PMO and assessed its immunoporotic potential. For assessing the same we employed three groups of adult C57BL/6 female mice that were randomly distributed into three groups: sham surgery (ovary intact), bilateral Ovx, and Ovx group orally administered with BC (10^9 cfu) per day for 8 weeks (Figure 3(a)). At the end of the treatment, mice were sacrificed, and the bones were collected for further studies. Interestingly, we observed that BC administration significantly improved the 3D-microarchitecture of proximal metaphysis of femoral region in Ovx mice (Figure 3(b)). Histomorphometric parameters indicated that BMD, bone volume/tissue volume (BV/TV) and trabecular thickness (Tb.Th) were significantly enhanced in Ovx mice administered with the BC (Figure 3(c–e)). In addition, trabecular separation (Tb.Sp) was found to be significantly reduced in Ovx + BC group (Figure 3(f)). These data demonstrate that BC administration significantly improves 3D microarchitecture and histomorphometric parameters of trabecular bones in osteoporotic mice.

BC promotes bone health via enhancing the anti-osteoclastogenic potential of Bregs

Our group had already established the anti-osteoporotic role of Breg-Treg cells and the osteoporotic role of Th17 cells in aggravating inflammatory bone loss in PMO.^{1,2,5} Thus, we next evaluated the frequencies of Breg, Treg, and Th17 cells population in various lymphoid organs (bone marrow-BM and spleen) in response to BC treatment in Ovx group. Interestingly, flow cytometry data revealed that CD19⁺CD1d^{hi}CD5⁺ Bregs population was significantly decreased in BM ($p < 0.01$) and spleen (p

menopausal osteoporosis-PMO). (i–k) Bar graph representing alpha diversity measures (Shannon Index, Simpson Reciprocal and Chao1) in human samples. (l) Spearman correlation between alpha diversity measures and femoral bone mineral density (BMD) in human samples. (m) Spearman correlation between alpha diversity measures and spine BMD in human samples. Data are expressed as mean \pm SEM. Data were analyzed by unpaired student t-test. * $p \leq 0.05$, ** $p \leq 0.01$, *** $p \leq 0.001$, **** $p \leq 0.0001$) compared with the indicated group.

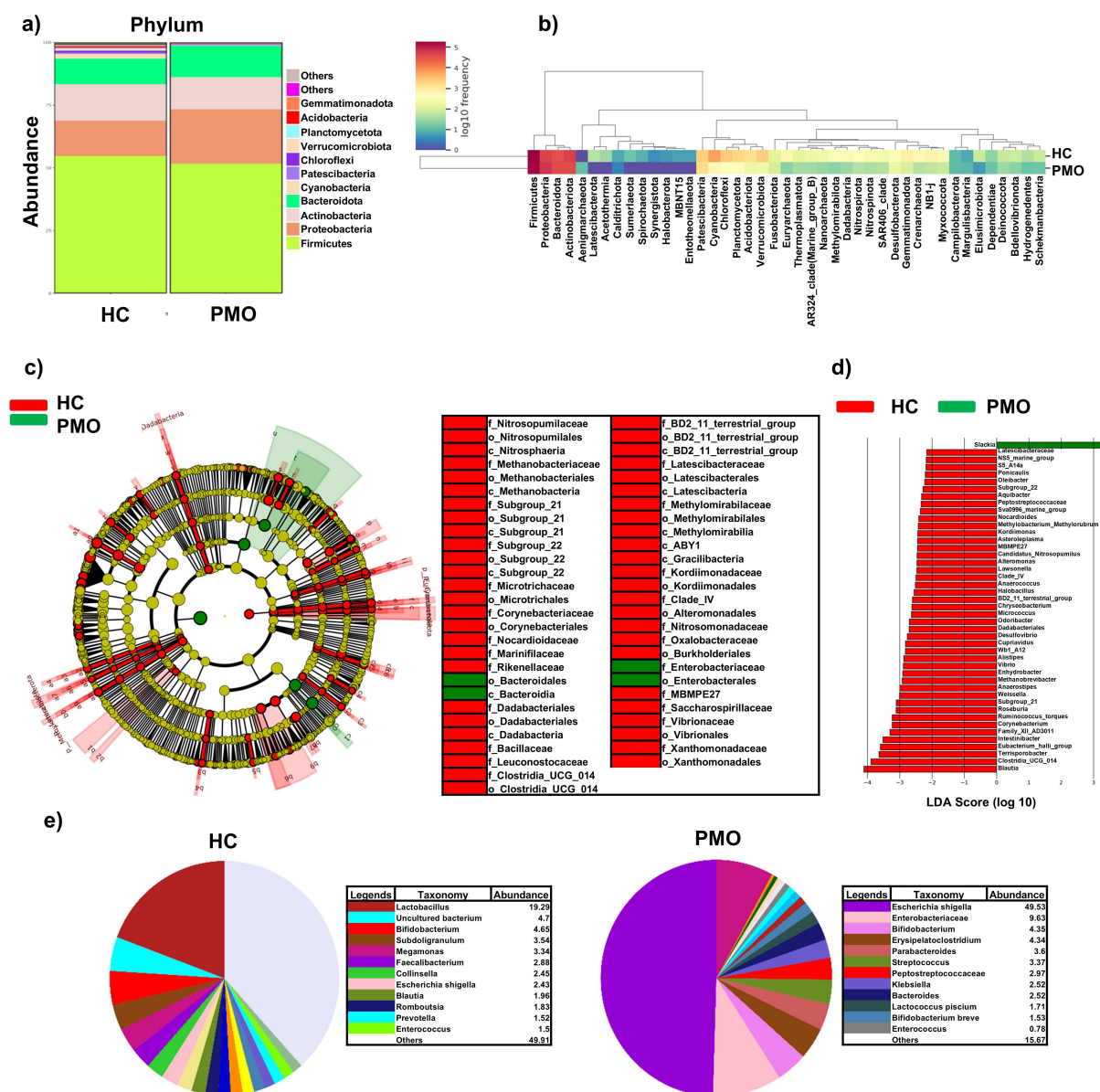


Figure 2. Dysbiosis of GM in the PMO patients: (a) Stacked bar chart representing the top 25 relative abundance of each phylum within each group in HC and PMO patients. (b) Heatmap denoting the dominant phylum in human samples. (c) LEfSe (linear discriminant analysis effect size) identifies microbiome differences at various phylogenetic levels. (d) LEfSe analysis with linear discriminant analysis (LDA) score representing statistical and biological differences in genera in between groups at genus level. (e) Pie chart and table representing the abundance of bacteria at species level in the HC and PMO patients.

< 0.01) of OvX mice compared with sham, and BC administration significantly increased the Bregs population in OvX group (Figure 4(a-c)). Of note, BC administration also significantly enhanced the frequencies of IL-10 producing Bregs (CD19⁺IL-10⁺) in OvX mice ($p < 0.05$) (Figure 4(d-f)). In addition, we further observed that the circulating levels of pro-osteoclastogenic cytokines viz. IL-6, TNF- α and IL-17 (signature cytokine of Th17 cells) and anti-osteoclastogenic cytokines viz.

IL-10 (signature cytokine of both Breg and Treg cells) and IFN- γ were significantly restored to homeostatic state in BC administered OvX group (Figure 4(g-k)). Since Bregs are functionally compromised under osteoporotic conditions,¹⁹ we next were interested in deciphering whether BC exhibit the potential to enhance the anti-osteoclastogenic potential of Bregs. For accomplishing the same, we isolated and differentiated Bregs independently from sham, OvX and OvX + BC mice and co-

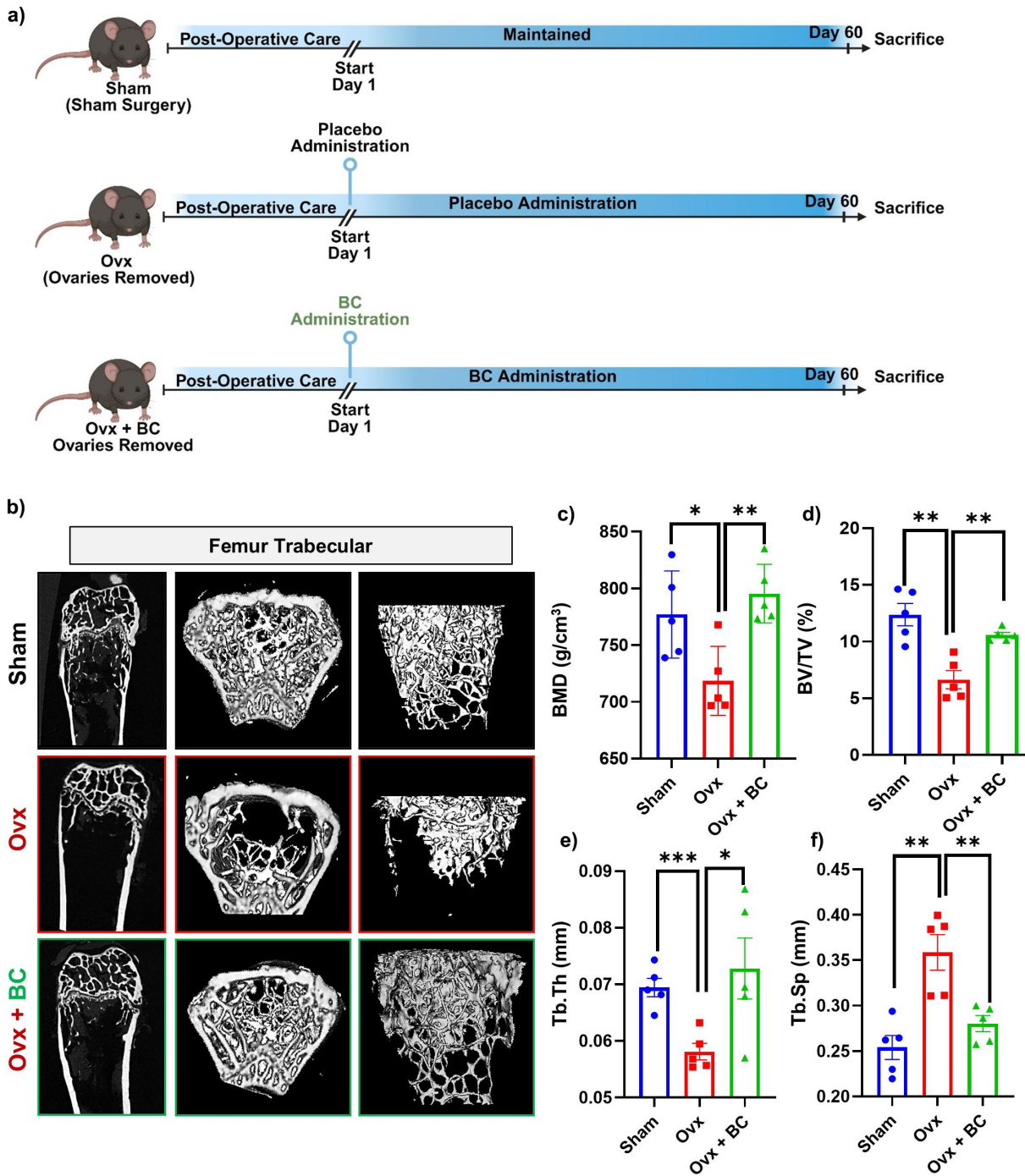


Figure 3. BC administration improves trabecular bone microarchitecture. (a) Schematic diagram depicting experimental design. (b) 3D μ CT reconstruction of femur trabecular of all groups. (c) Bone microarchitecture of femur trabecular. (d) Bone mineral density (BMD). (e) Bone volume/Tissue volume (BV/TV). (f) Trabecular thickness (Tb.Th). (g) Trabecular separation (Tb.Sp). The results were evaluated by one way ANOVA with subsequent comparisons by Student t-test for paired or unpaired data. Values are reported as mean \pm SEM ($n = 5$). Statistical significance was considered as $p \leq 0.05$ (* $p \leq 0.05$, ** $p \leq 0.001$, *** $p \leq 0.0001$) with respect to indicated mice groups.

cultured them with osteoclasts precursors (isolated from sham animals) at 1:1 cell ratio. Remarkably, we observed that Bregs harvested from the sham and Ovx + BC group significantly reduced the differentiation of multinucleated TRAP positive

osteoclasts (Figure 5(a–b)). On the contrary, Ovx-Bregs were inefficient in inhibiting osteoclastogenesis, as demonstrated by the enhanced number and area of multinucleated TRAP positive osteoclasts (Figure 5(a–e)). Of note, we observed that Bregs

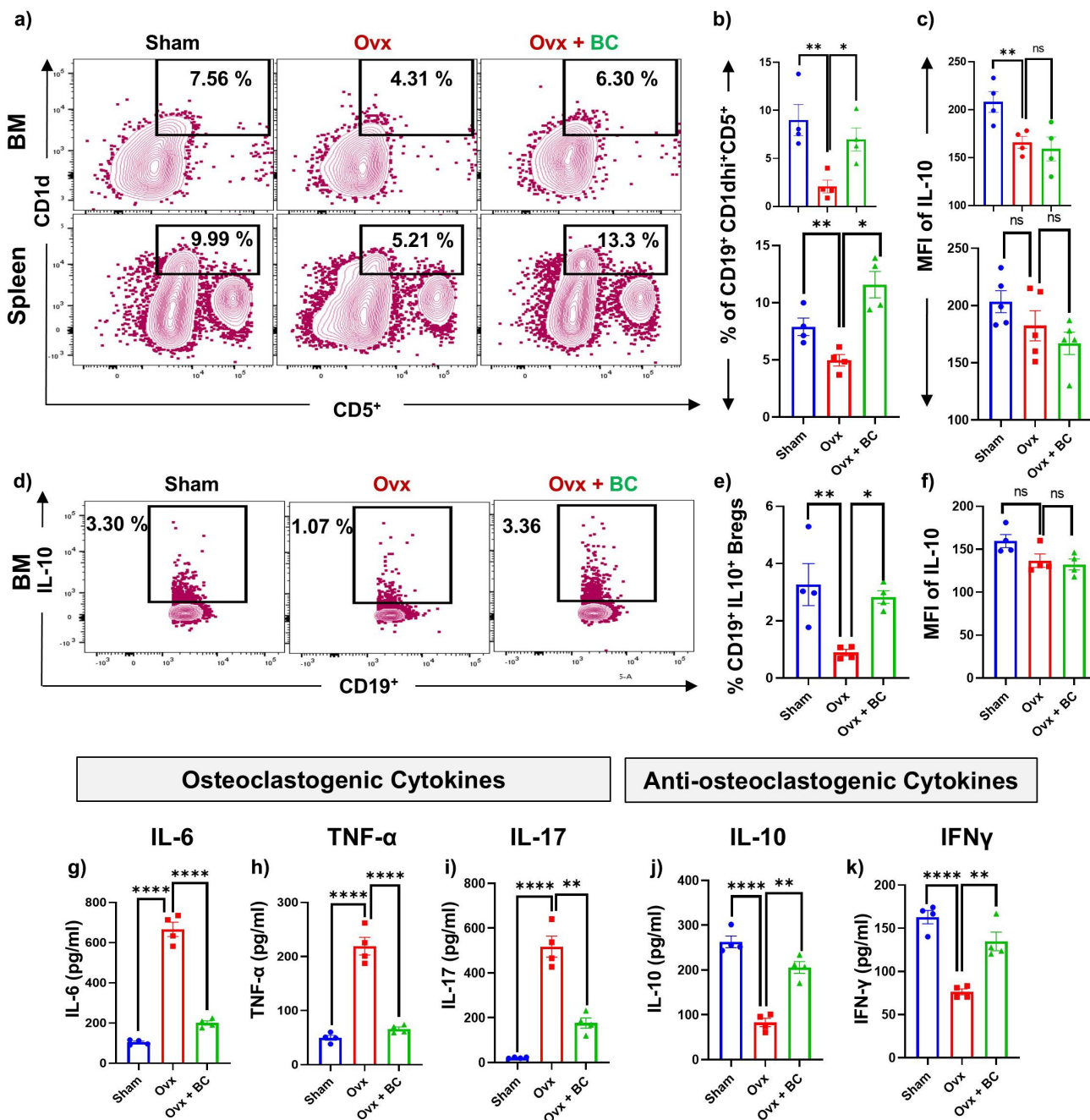


Figure 4. BC administration modulates Bregs in Ovx mice: (a) Contour plot representing percentage of Bregs in BM and spleen. (b) Bar graphs depicting percentage of Bregs in BM and spleen. (c) Bar graphs representing mean fluorescence intensity (MFI) of IL-10 in Bregs within BM and spleen. (d) Total CD19⁺IL-10⁺ Bregs. (e) Bar graphs representing CD19⁺IL-10⁺ Bregs. (f) MFI of IL-10. (g-k) Osteoclastogenic and anti-osteoclastogenic cytokines were analyzed in serum samples of mice by ELISA. The results were evaluated by one way ANOVA with subsequent comparisons by Student t-test for paired or unpaired data. Values are reported as mean \pm SEM ($n = 4$). Statistical significance was considered as $p \leq 0.05$ (* $p \leq 0.05$, ** $p \leq 0.01$, *** $p \leq 0.0001$) with respect to indicated mice groups.

harvested from the Ovx + BC mice group have significantly enhanced anti-osteoclastogenic potential as evidenced by reduced number and area of multinucleated TRAP positive osteoclasts (Figure 5(c-e)).

This data unequivocally demonstrated that BC administration augments the anti-osteoclastogenic potential of Bregs in addition to the enhanced frequencies of Bregs in Ovx mice.

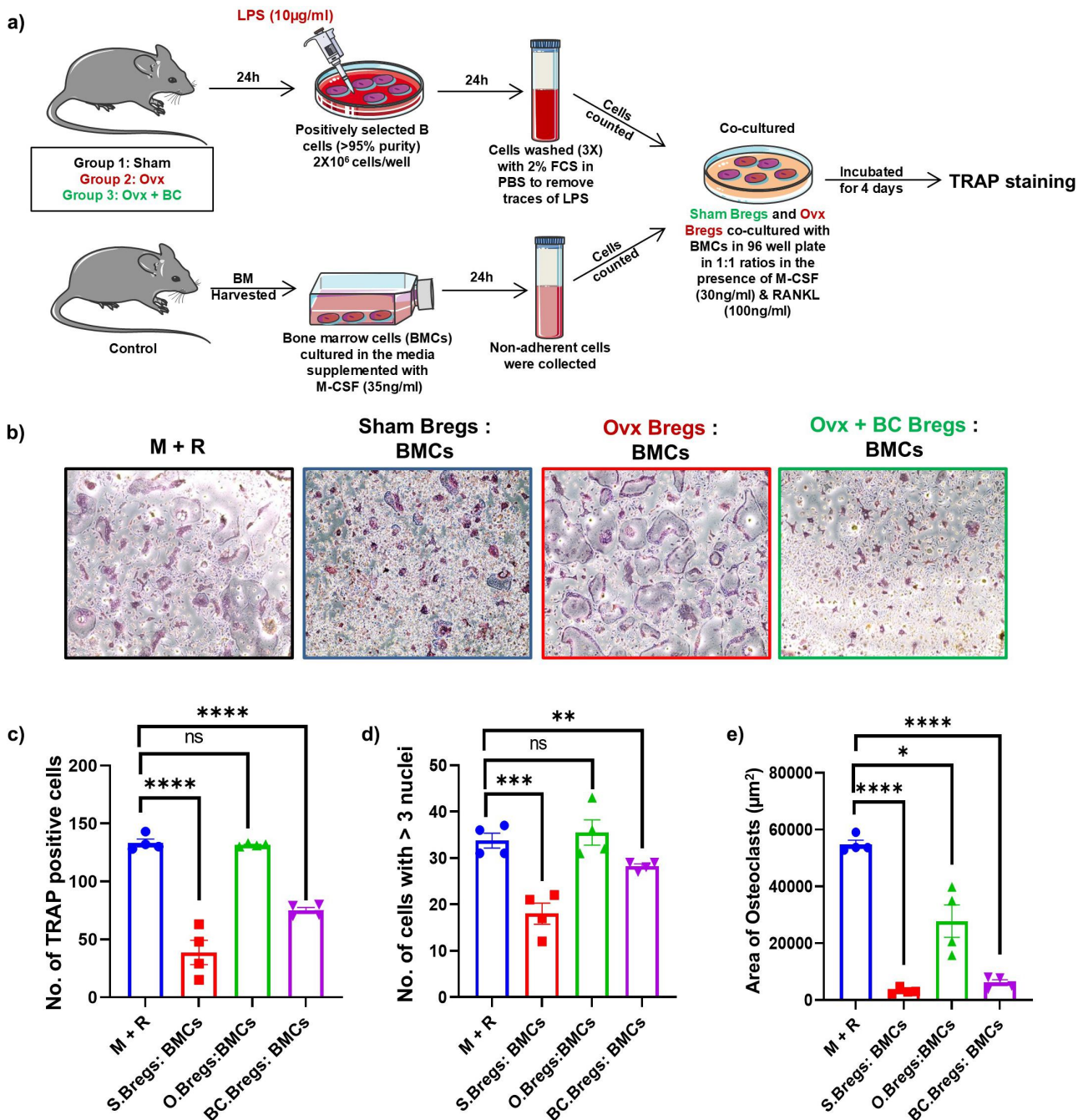


Figure 5. BC enhances the anti-osteoclastogenic potential of Bregs : (a) Experimental layout followed for the co-culture of Bregs and BMCs. (b) Photomicrographs (10X magnification) representing TRAP positive multinucleated osteoclasts. (c) Number of TRAP positive cells. (d) Number of osteoclasts with more than 3 nuclei. (e) Area of osteoclasts. The results were evaluated by one way ANOVA with subsequent comparisons by Student t-test for paired or unpaired data. Values are reported as mean \pm SEM. Statistical significance was considered as $p \leq 0.05$ (* $p \leq 0.05$, ** $p \leq 0.001$, *** $p \leq 0.0001$) with respect to indicated mice groups.

BC administration enhances the immunosuppressive and immunomodulatory potential of Bregs in Ovx mice

With the intent to decipher the role of BC on Breg's immunomodulatory potential, we next co-cultured

Bregs isolated from sham, Ovx and Ovx + BC mice with CFSE labeled naïve CD4⁺CD25⁻ effector T cells at 1:1 cell ratio in the presence of anti-CD3 and anti-CD28 mAbs. The proliferation of effector T cells was measured and quantified by

the dilution of CFSE fluorescence (Figure 6(a)). We observed that sham-Bregs significantly suppressed the proliferation of effector T cells, indicated by their high proliferation index (Figure 6(b-e)). On the contrary, Ovx-Bregs were unable to suppress the proliferation of $CD4^+CD25^-$ effector T cells (Figure 6(b-e)). Remarkably, Bregs isolated from

Ovx + BC group had enhanced immunosuppressive potential as they were able to drastically reduce the proliferation of effector T cells under *ex vivo* conditions in comparison to the Ovx Bregs (Figure 6(b-e)).

Strikingly, we further observed that Ovx-Bregs have compromised immunomodulatory

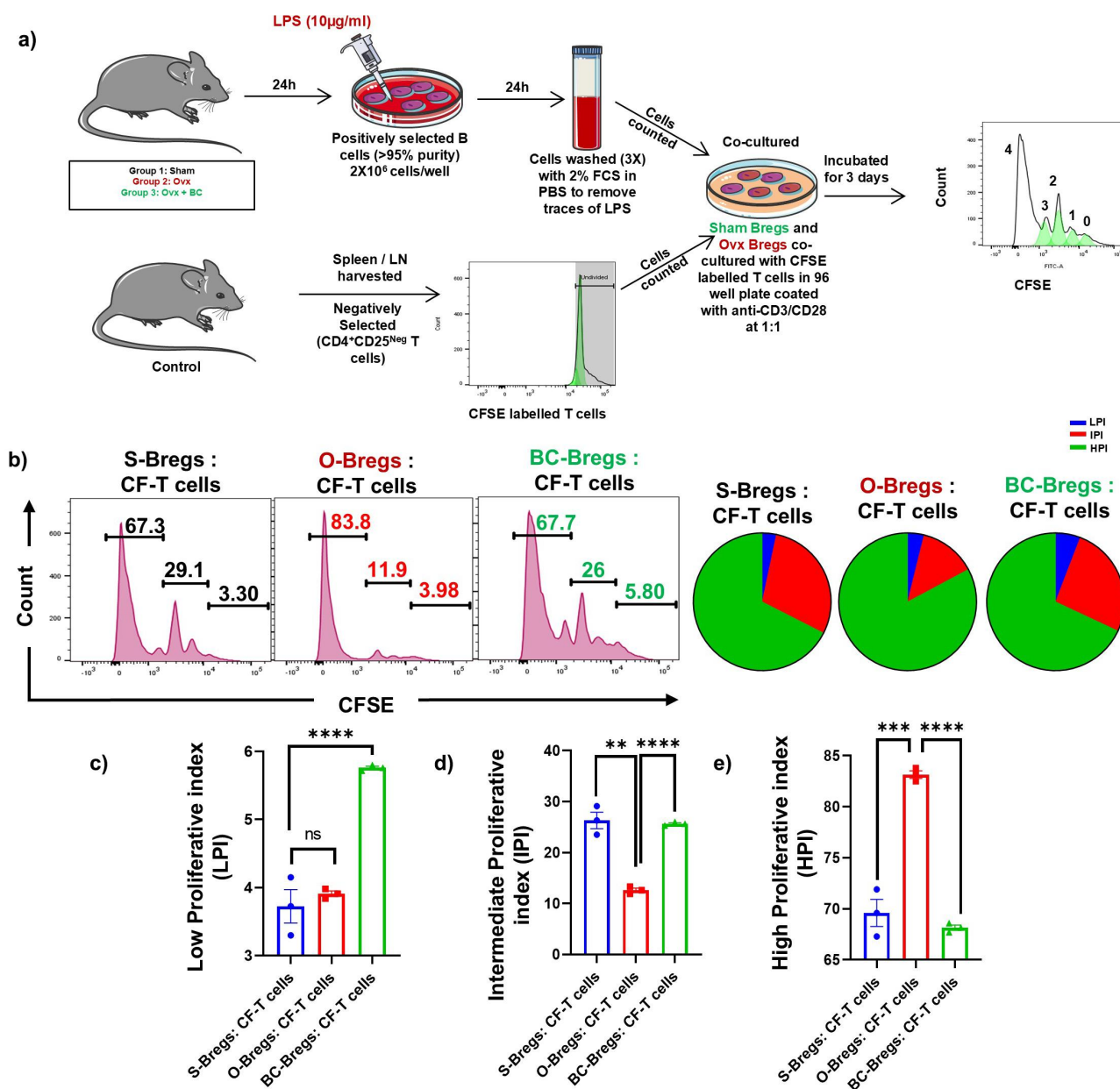


Figure 6. BC enhances the immunosuppressive potential of Bregs in Ovx mice: (a) Experimental layout followed for the co-culture of Bregs generated from $CD19^+$ B cells of sham, Ovx and Ovx + BC mice with CFSE labeled T cells. (b) Histograms and pie charts representing percentage of proliferative CFSE labeled T cells in different conditions. (c) Bar graphs representing low proliferative index (LPI). (d) Bar graphs representing intermediate proliferative index (IPI). (e) Bar graphs representing high proliferative index (HPI). The results were evaluated by one way ANOVA with subsequent comparisons by Student t-test for paired or unpaired data. Values are reported as mean \pm SEM. Statistical significance was considered as $p \leq 0.05$ (* $p \leq 0.05$, ** $p \leq 0.001$, *** $p \leq 0.0001$) with respect to indicated mice groups.

functions, as evidenced by their reduced capacity to induce the differentiation of Tregs ($CD4^{+}Foxp3^{+}$) along with suppressing Th17 cell ($CD4^{+}Roryt^{+}$) differentiation (Figure 7(a–e)). Interestingly, we observed that Bregs harvested from the Ovx + BC group significantly enhanced the differentiation of naïve T cells to

Tregs, along with concomitantly reducing the differentiation of naïve T cells to Th17 cells (Figure 7(a–e)). In addition, the percentages of anti-osteoclastogenic $CD4^{+}Foxp3^{+}$ Tregs in BM ($p < 0.01$) and spleen ($p < 0.01$) in the Ovx group were lower than the sham, and BC treatment significantly restored the frequencies of Tregs in Ovx + BC group

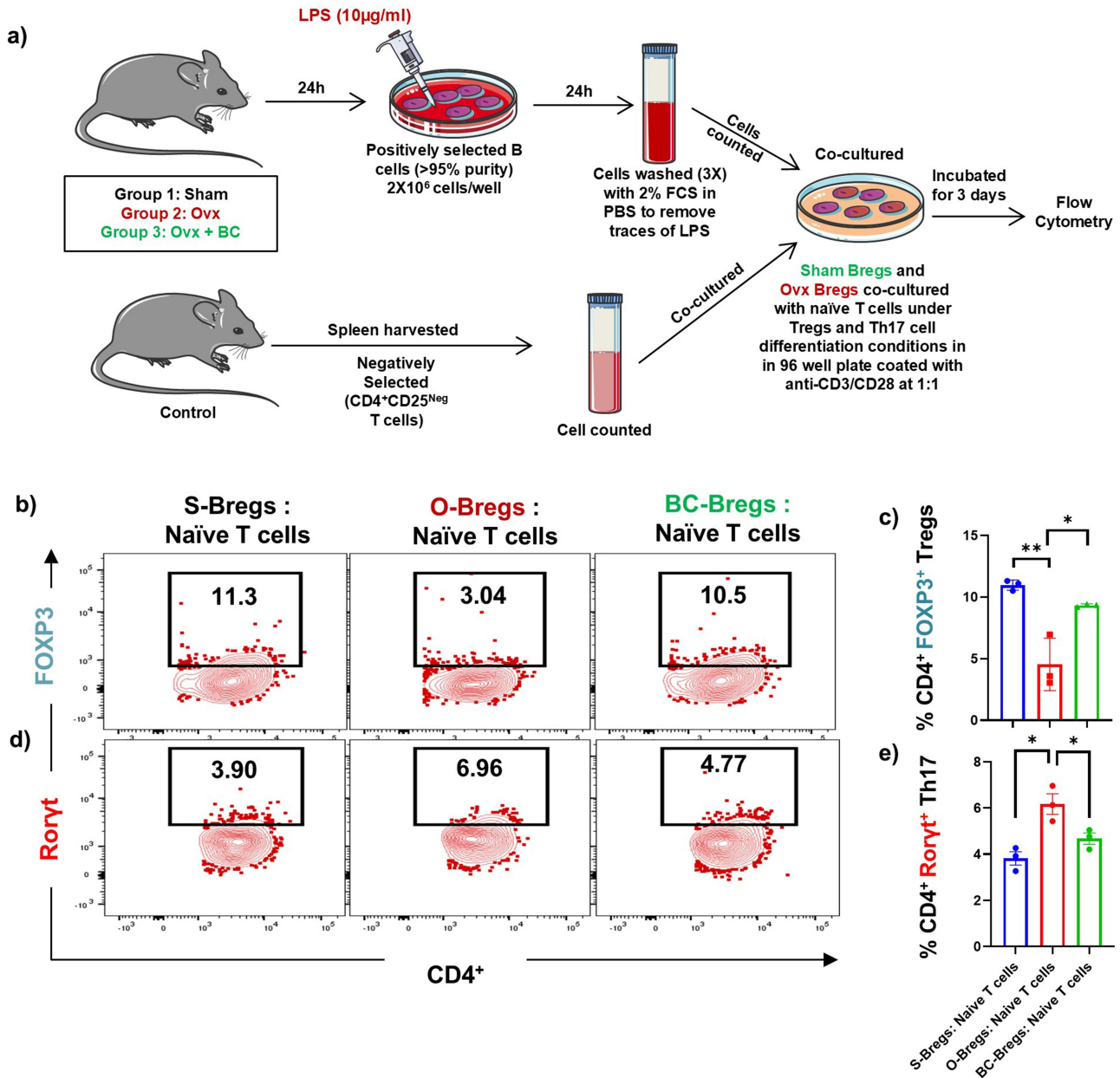


Figure 7. BC administration enhance the inherent immunomodulatory potential of Bregs in Ovx mice: (a) Experimental layout followed for the co-culture of co-culture of Bregs generated from $CD19^{+}$ B cells of Sham, Ovx and Ovx + BC mice with naïve T cells. (b) Contour plots representing percentage of $CD4^{+}Foxp3^{+}$ Tregs co-cultured with S-Bregs, O-Bregs and BC-Bregs. (c) Bar graphs representing percentage of $CD4^{+}Foxp3^{+}$ Tregs. (d) Contour plots representing percentage of $CD4^{+}IL-17^{+}$ Th17 cells co-cultured with S-Bregs, O-Bregs and BC-Bregs. (e) Bar graphs representing percentage of $CD4^{+}IL-17^{+}$ Th17 cells. The results were evaluated by one way ANOVA with subsequent comparisons by Student t-test for paired or unpaired data. Values are reported as mean \pm SEM. Statistical significance was considered as $p \leq 0.05$ (* $p \leq 0.05$, ** $p \leq 0.001$, *** $p \leq 0.0001$) with respect to indicated mice groups.

(Figure S3a-d). Conversely, we observed that Ovx mice had significantly higher percentages of osteoclastogenic CD4⁺Roryt⁺ Th17 cells in BM ($p < 0.001$) and spleen ($p < 0.001$), and BC treatment significantly reduced Th17 cell population in Ovx group (Figure S4a-d). These results, clearly suggest that BC via enhancing the anti-osteoclastogenic and immunomodulatory potential of Bregs further complements the amelioration of inflammatory bone loss observed in PMO.

BC enhances gut integrity via modulating the “Breg-Treg-Th17” cell axis in gut associated lymphoid tissue (GALT)

Findings from our group and others have already established the nexus between “GUT-Immune-Bone” axis.^{7,8,20} Interestingly, we observed that apart from modulating the frequencies of Bregs, Tregs and Th17 cells in the BM and spleen, BC administration also modulated the dysregulated “Breg-Treg-Th17” cell axis in the gut associated lymphoid tissue (GALTs, viz. Peyer’s patches-PP) in Ovx mice (Figure 8(d-l)). Thus, moving ahead, we proposed that BC administration modulates the frequencies of both regulatory (Breg and Treg) and inflammatory (Th17) cells in the GALTs thereby preserving gut-barrier integrity and bone health. Notably, the colon length (indicative of inflamed gut) was observed to be significantly reduced in the Ovx group and supplementation of BC significantly preserved the same (Figure 8(a-b)). Next, we explored the effect of BC administration on gut permeability. Of note, we observed that BC supplementation significantly reduced the gut-leakiness and maintains gut-barrier functions as evidenced by the reduced leakage of FITC-Dextran (high fluorescence intensity) in the peripheral circulation of Ovx mice (Figure 8(c)). Altogether, our results clearly suggest that BC ameliorates inflammatory bone loss via modulating the “Gut-Bone-Immune” axis.

BC via enhancing SCFAs dampens inflammatory bone loss in Ovx mice

To decrypt the underlying mechanism via which BC impart their bone health promoting effects, we next carried out targeted metabolomics

for the analysis of SCFAs in the fecal samples of different groups (Figure 9(a)). Interestingly, HPLC data demonstrated that Ovx mice have significantly reduced amounts of SCFAs (viz. acetate, butyrate and propionate) in the fecal samples as compared to the control group (Figure 9(b)), suggesting toward the potential involvement of SCFAs in modulating bone health under estrogen deficient conditions. Strikingly, our HPLC data further revealed that BC indeed mediated its immunoporotic (immunomodulatory and osteoprotective) effects even under estrogen deficient conditions via enhancing the production of SCFAs in the gut. It was observed that supplementation of BC significantly enhanced the concentrations of acetate, propionate, and butyrate in the Ovx mice (Figure 9(b)). This data robustly indicated that BC ameliorates inflammatory bone loss via enhancing the production of SCFAs in the gut, even under estrogen deficient conditions.

SCFAs inhibit osteoclastogenesis

Moving ahead we next evaluated the role of SCFAs on RANKL induced osteoclastogenesis under *ex vivo* conditions. For achieving the same, BMCs were stimulated with osteoclastogenic media supplemented with M-CSF (30 ng/ml) and RANKL (100 ng/ml) in the presence or absence of SCFAs at different concentrations (0.125 mM, 0.25 mM, and 0.5 mM). After 4 days, cells were harvested and processed for TRAP staining. Interesting, we observed a significant reduction in the differentiation of osteoclasts in a dose-dependent manner as evident by a significant reduction in multinucleated (>3 nuclei) TRAP-positive cells in SCFAs treated group in comparison to control group (Figure 9(c-d)). Furthermore, the area of multinucleated osteoclasts in treatment groups was significantly reduced as compared to the control group (Figure 9(d)). To eliminate the likelihood that the observed lessening in osteoclasts differentiation and number is not due to cell cytotoxicity, MTT assay was performed, and we found no significant difference in cell viability with SCFAs treatment at different concentrations (data not shown). These results clearly suggest that SCFAs have the potential to inhibit RANKL-induced osteoclastogenesis.

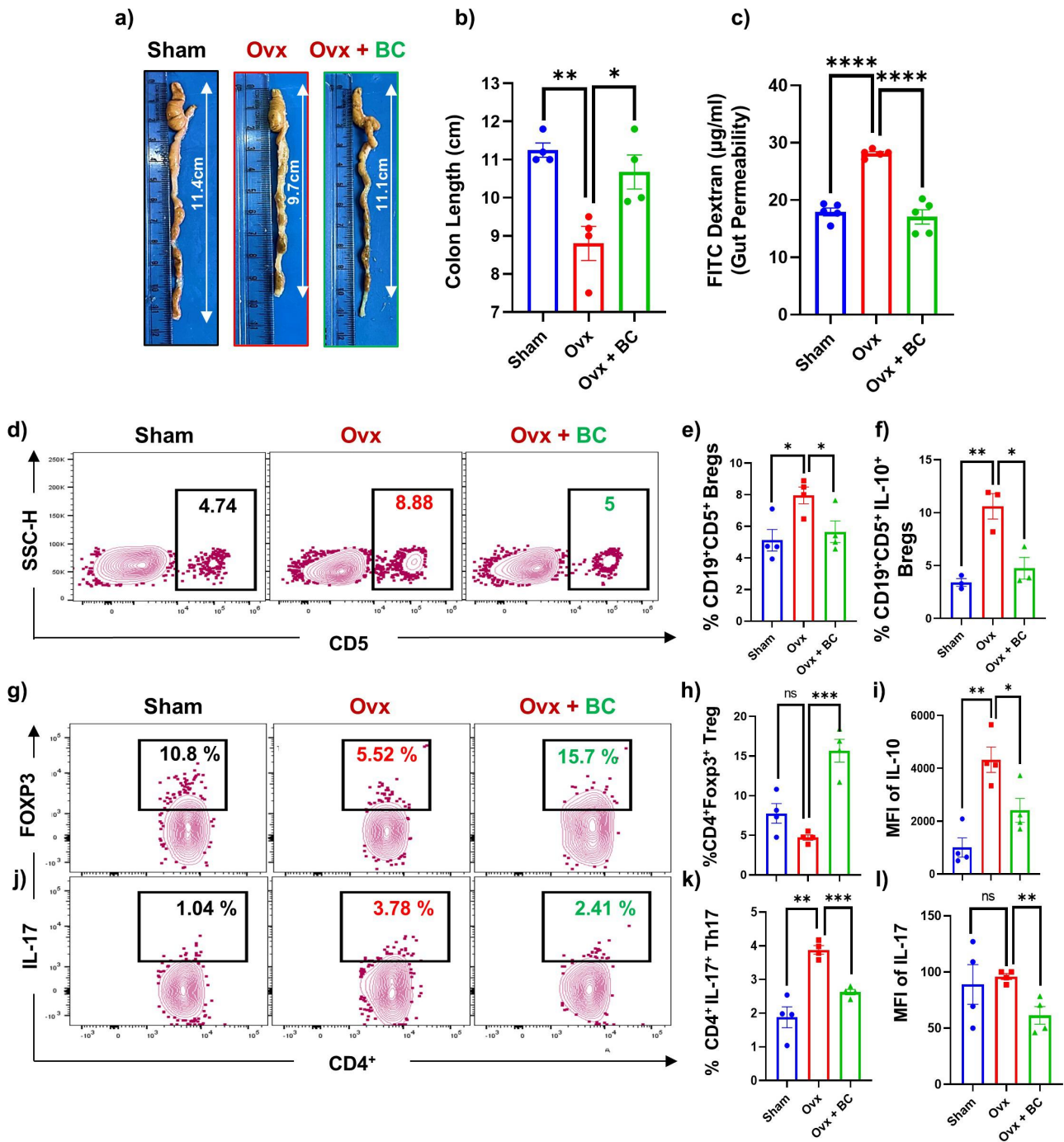


Figure 8. BC enhances gut integrity via modulating the “Breg-Treg-Th17” cell axis in GALT (PP): (a) Colon length of sham, OvX and OvX + BC mice. (b) Bar graphs representing colon length. (c) Bar graphs representing intestinal permeability in OvX mice. (d) Contour plots depicting percentage of CD19⁺CD5⁺ Bregs in PP. (e) Bar graphs depicting percentage of CD19⁺CD5⁺ Bregs in PP. (f) Bar graphs representing percentage of CD19⁺CD5⁺IL-10⁺ Bregs. (g) Contour plot representing percentage of CD4⁺FOXP3⁺ Tregs in PP. (h) Bar graphs representing percentage of CD4⁺FOXP3⁺ Tregs in PP. (i) MFI of IL-10. (j) Contour plots depicting percentage of CD4⁺IL-17⁺ Th17 cells. (k) Bar graphs representing percentage of CD4⁺IL-17⁺ Th17 cells. (l) MFI of IL-17. The results were evaluated by using ANOVA with subsequent comparisons by Student t-test for paired or unpaired data, as appropriate. Values are expressed as mean \pm SEM ($n = 3$ or 4) and similar results were obtained in two independent experiments. Statistical significance was considered as $p \leq 0.05$ (* $p \leq 0.05$, ** $p \leq 0.01$, *** $p \leq 0.0001$) with respect to indicated mice groups.

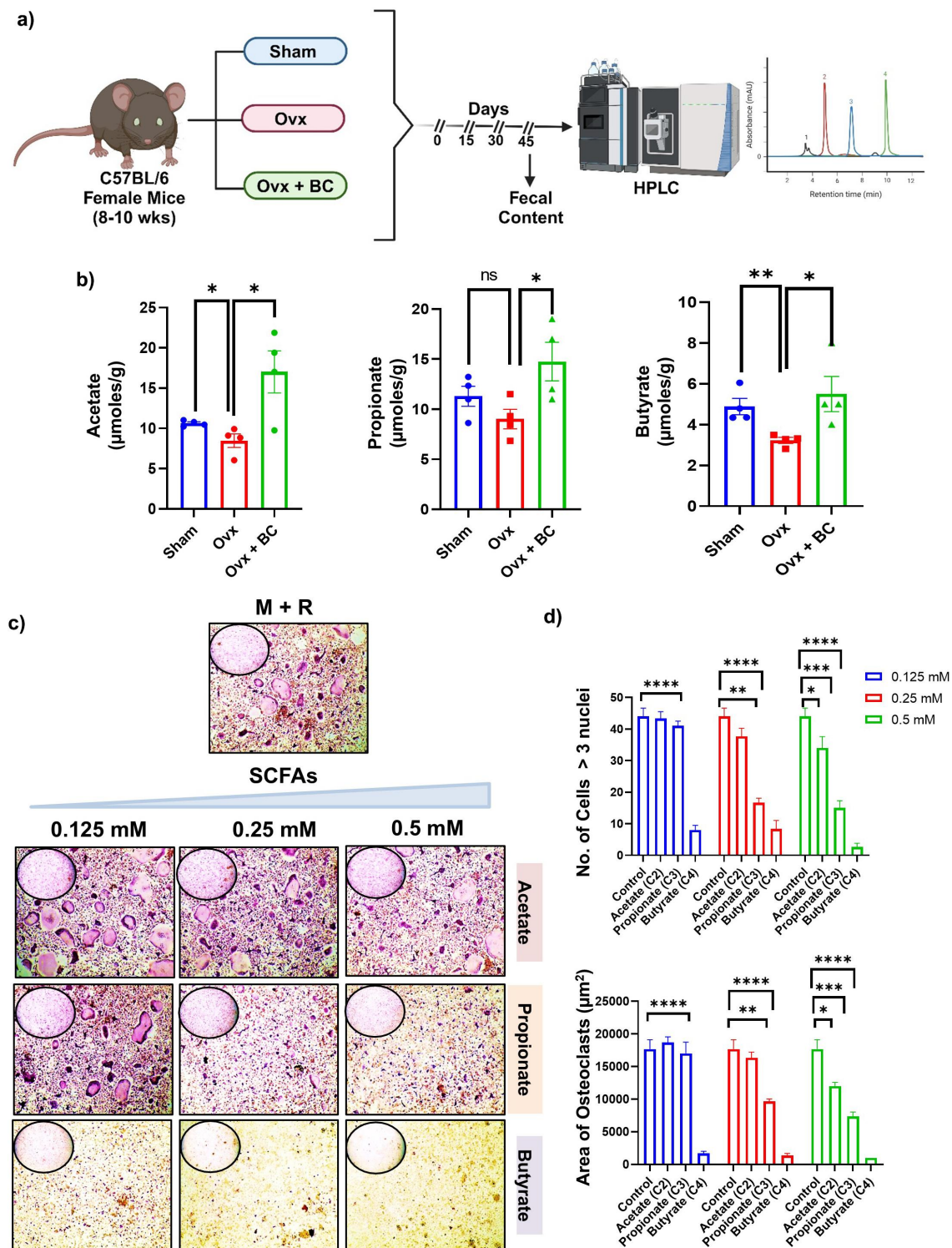


Figure 9. BC via enhancing SCFAs inhibits osteoclasts differentiation in Ovx mice: (a) For SCFAs analysis, mice were divided into 3 groups. viz. Sham, Ovx and Ovx + BC. At the end of 45 days, fecal samples are collected from all the groups of mice and analyzed for short chain fatty acids (SCFAs) with the help of high-performance liquid chromatography (HPLC). (b) Bar graphs representing the concentration of acetate, propionate, and butyrate in fecal samples of sham, Ovx, and Ovx + BC groups. (c) Photomicrographs (10X magnification) representing TRAP positive cells. (d) Number of TRAP positive cells with more than 3 nuclei and area of osteoclasts. Data are expressed as mean \pm SEM. Data were analyzed by unpaired student t test and analyzed by one way ANOVA. * $p \leq 0.05$, ** $p \leq 0.01$, *** $p \leq 0.001$, **** $p \leq 0.0001$ compared with the indicated group.

SCFAs modulates “Breg-Treg-Th17” cell axis

BC exhibit strong immunomodulatory potential; thus, we were next estimated the potential of SCFAs on the differentiation of Breg, Treg and Th17 cells. For the same, negatively selected splenic B cells were stimulated under Breg polarizing conditions in the presence/absence of SCFAs (viz. acetate, propionate and butyrate) for 24 h (Figure 10(a–d)). It was observed that SCFAs significantly enhanced the percentage of CD19⁺IL-10⁺ Bregs under *ex vivo* conditions in a concentration dependent manner (Figure 10(a–d)). Next, we assessed the potential of SCFAs on the differentiation of naïve T cells either into Tregs or Th17 cells. To achieve this aim, we cultured naïve T cells with SCFAs for 3 days under Tregs and Th17 cell differentiation conditions respectively. Subsequently, cells were harvested and analyzed for the percentages of CD4⁺Foxp3⁺ Tregs and CD4⁺Roryt⁺ Th17 cells by flow cytometry. Interestingly, we observed that among all SCFAs, butyrate was the most efficient in significantly reducing the differentiation of naïve T cells to CD4⁺Roryt⁺ Th17 cells ($p < 0.0001$) in comparison to control groups (Figure 10(e–f)). In addition, butyrate (at 0.5 mM concentration) was also able to significantly enhance the differentiation of naïve T cells to CD4⁺Foxp3⁺ Tregs ($p < 0.001$) under *ex vivo* conditions (Figure 10(g–h)). Conclusively, this data clearly supports that among all the SCFAs, butyrate is the most potent in modulating the differentiation of Breg, Treg and Th17 cells, along with inhibiting osteoclastogenesis.

Butyrate enhances bone health via modulating the “Gut-Immune” axis

To test whether our above *ex vivo* findings of butyrate could be exploited as a novel therapeutic strategy in the treatment of pathological bone loss conditions, we next investigated the role of butyrate in modulating bone health under estrogen deficient conditions in OvX mice model. For the same, adult C57BL/6 female mice were randomly distributed into three groups: sham surgery, bilateral OvX, and OvX group orally administered daily with butyrate (150 mM) for 6 weeks. At the end of

the treatment, mice were sacrificed and various osteoimmune parameters were analyzed (Figure 11(a)). Micro-CT analysis further denoted improved 3D microarchitecture of LV-5 bone of OvX mice administered with butyrate (Figure 11(a)). Also, butyrate administration significantly enhanced the BMD of femoral and LV-5 bones in OvX group (Figure 11(a–c)). In addition, to the improved bone microarchitecture, butyrate administration also enhanced the mechanical strength of the femoral bone in OvX + butyrate group as compared to OvX group, as evidenced by the significant enhancement in the energy required to break the bone (Figure 11(d)). We next explored the potential of butyrate administration on gut-permeability. Of note, we observed that butyrate supplementation significantly reduced the leakiness in the gut and maintains the gut barrier function in OvX mice (Figure 11(e)). In addition, our flow cytometric data further demonstrated that butyrate supplementation significantly enhanced the frequencies of Bregs and Tregs along with simultaneously reducing the frequencies of Th17 cells in BM (prime site of osteoclastogenesis) (Figure 11(f–i)). Altogether, our above data confirms that BC enhances bone health under PMO conditions in an SCFA dependent manner (viz. butyrate) via modulating the gut-immune axis.

SCFAs inhibit osteoclastogenesis in PBMCs of PMO patients

Moving ahead, we were keen to know whether SCFAs can dampen the inflammatory bone loss in healthy and PMO patients. For the same we next carried out osteoclastogenic assay in both healthy control and PMO patients. We examined the potential of SCFAs on RANKL mediated osteoclastogenesis in the presence or absence of SCFAs at 0.5 mM concentration in PBMCs of HC and PMO subjects. After 14 days, cells were harvested and processed for TRAP staining. Reduction in the differentiation of osteoclasts as evident by a significant reduction in multinucleated (>3 nuclei) TRAP-positive cells in SCFAs treated group in both HC and PMO patients (Figure 12(a–c)) was observed. This data undoubtedly demonstrated that among all SCFAs, butyrate was most potent in suppressing osteoclastogenesis in both HC and PMO patients, thereby further validating our pre-clinical

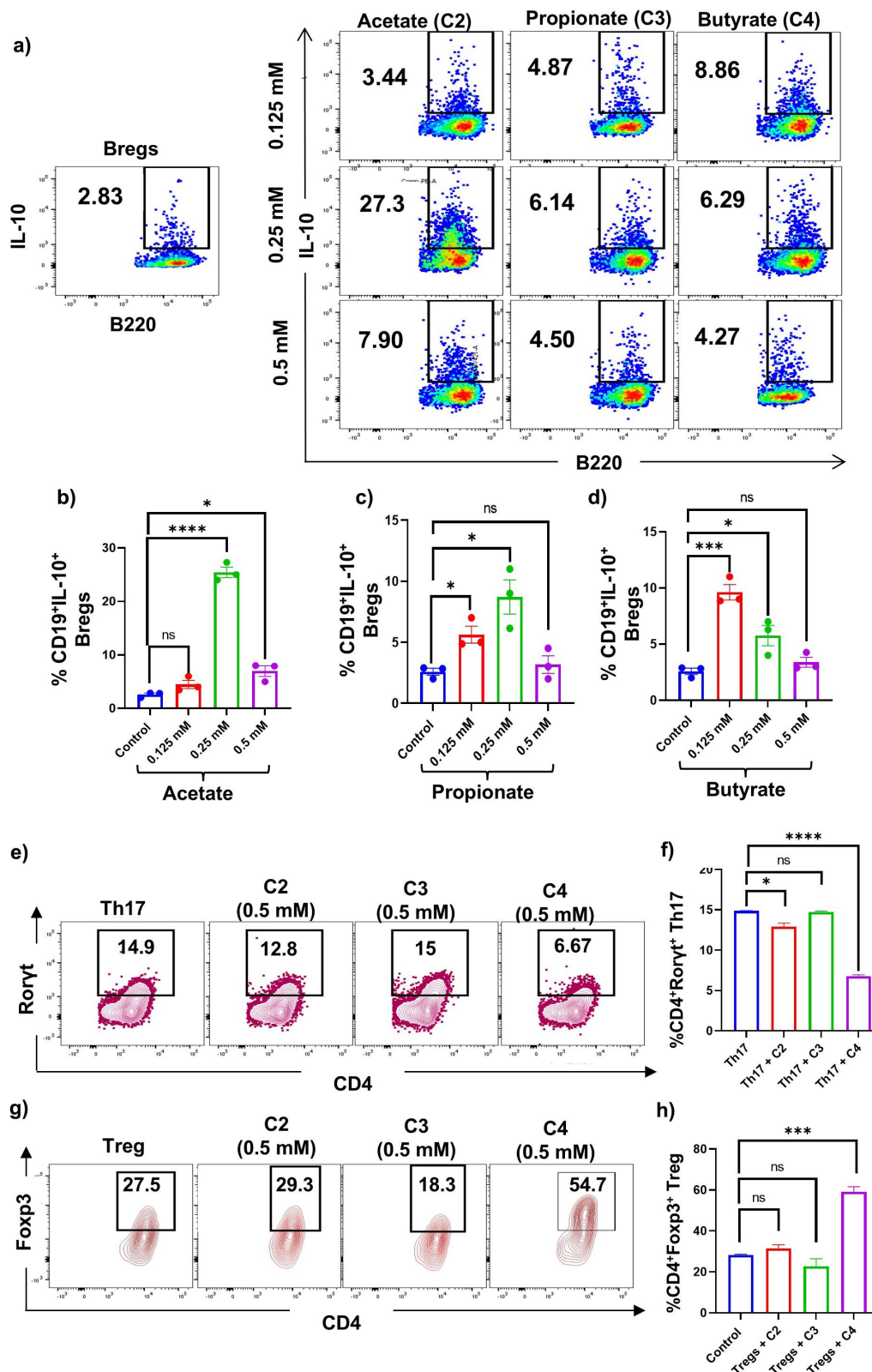


Figure 10. SCFAs enhance the immunomodulatory potential of Bregs: (a-d) for Bregs stimulation, splenic CD19⁺ B cells were negatively selected and stimulated with LPS (10 μ g/ml) in the presence and absence of SCFAs at different concentrations. Dot plots and bar graphs depicting the percentages of CD19⁺IL-10⁺ Bregs. (e-f) Contour plots and bar graphs are representing frequencies of Th17 cells in the presence and absence of SCFAs at different concentrations. (g-h) Contour plot and bar graphs are representing frequencies of Treg in the presence and absence of SCFAs at different concentrations. Data is represented as mean \pm SEM. Similar results were obtained in two different independent experiments. Statistical significance was considered as $p \leq 0.05$ (* $p \leq 0.05$, ** $p \leq 0.01$, *** $p \leq 0.001$) with respect to indicated groups.

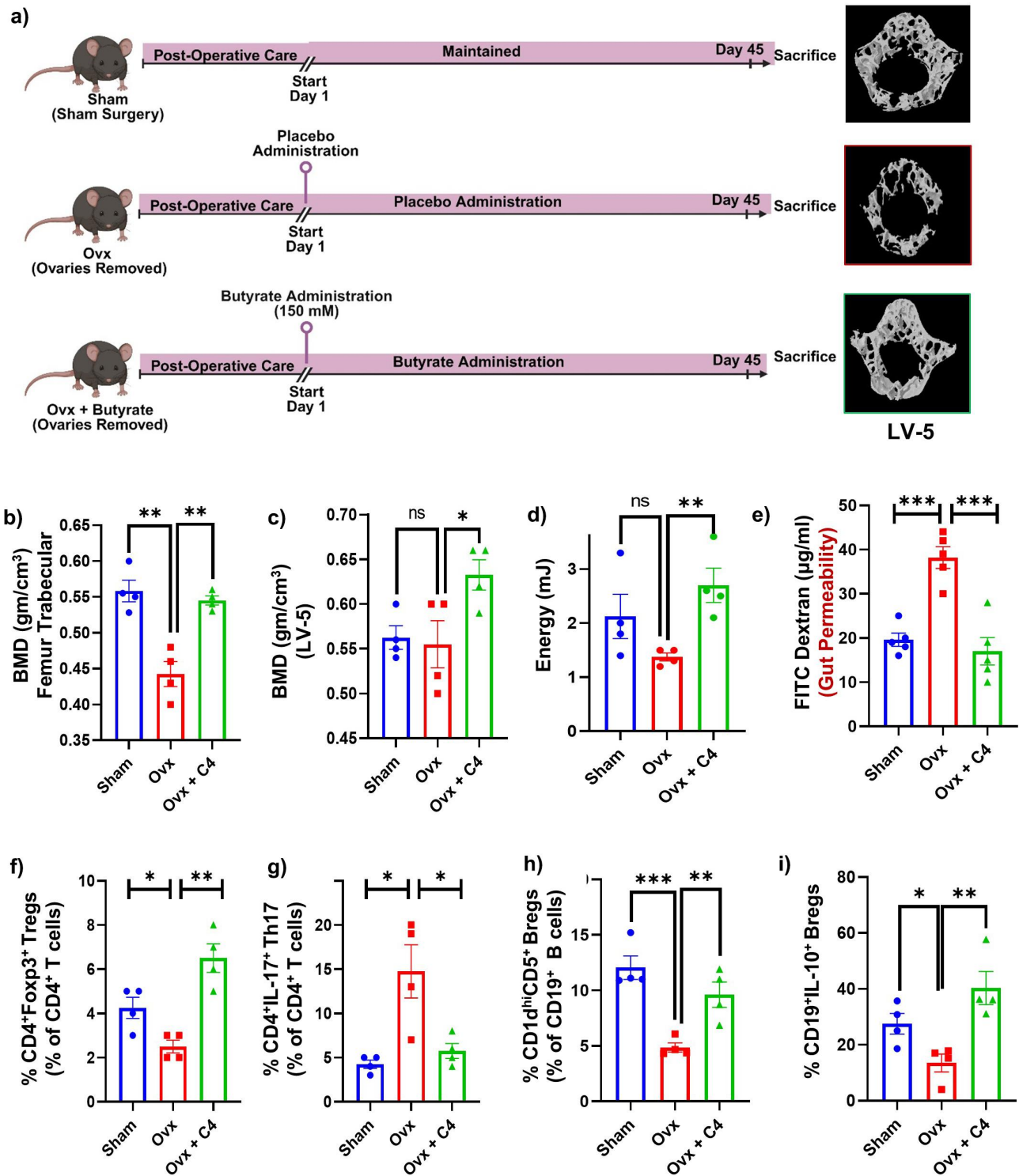


Figure 11. Butyrate enhances bone health via modulating the “Breg-Treg-Th17” cell axis and gut integrity: (a) Experimental layout followed for the *in vivo* studies. (b) BMD of femoral trabecular bone. (c) BMD of LV-5 trabecular bone. (d) Bar graph representing energy. (e) Measurement of gut integrity. FITC dextran was administered orally to each experimental mouse. Fluorescence intensity was measured at excitation: 488 nm and 528 nm emission as an indicative of gut integrity. (f) Frequencies of Tregs. (g) Frequencies of Th17 cells. (h) Frequencies of CD19⁺CD1d^{hi}CD5⁺ Bregs. (i) Frequencies of CD19⁺IL-10⁺ Bregs in the BM of mice of different groups. Data is represented as mean \pm SEM ($n = 4$). Similar results were obtained in two different independent experiments. Statistical significance was considered as $p \leq 0.05$ (* $p \leq 0.05$, ** $p \leq 0.01$, *** $p \leq 0.001$) with respect to indicated groups.

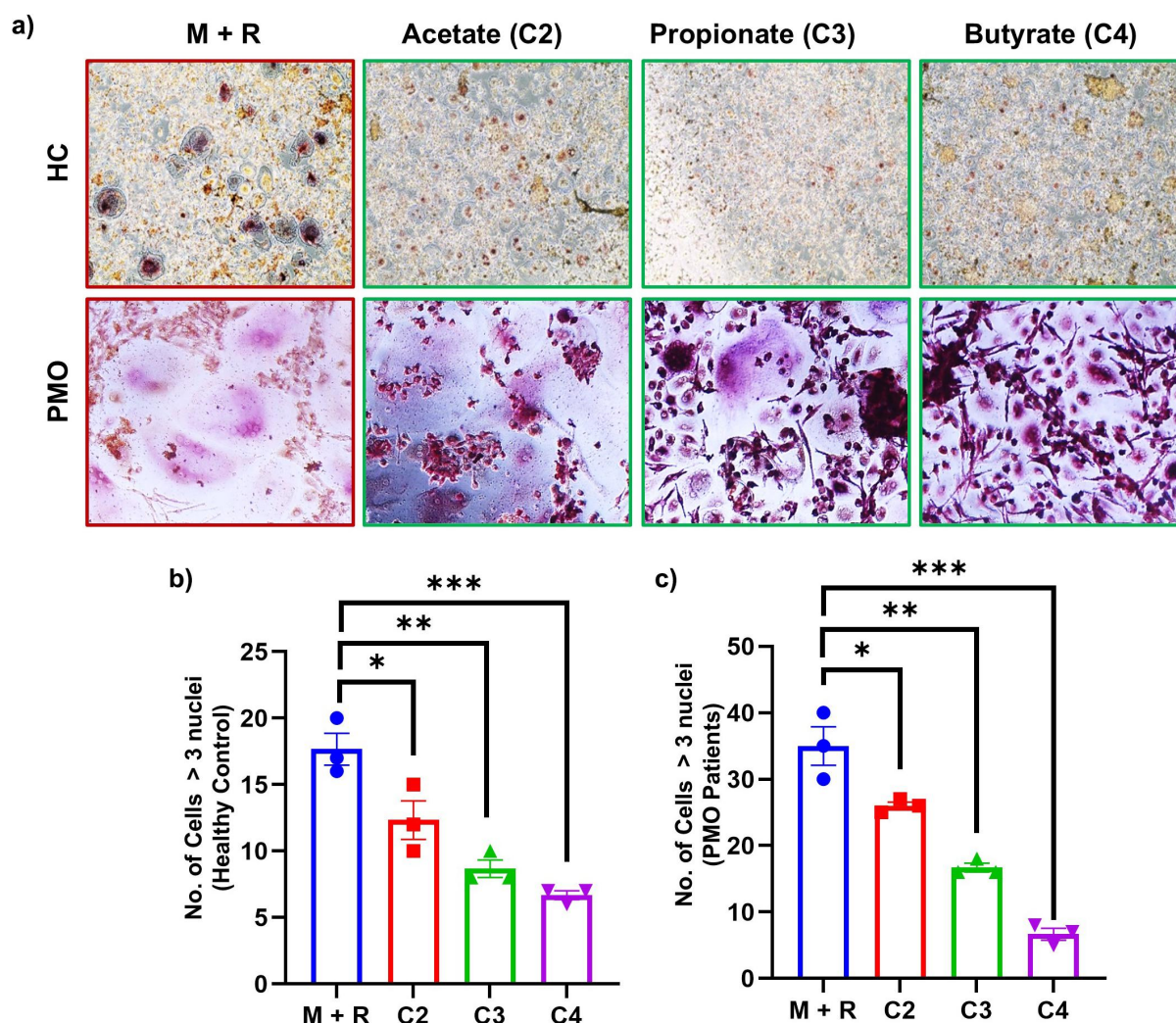


Figure 12. SCFAs inhibits osteoclastogenesis in PBMCs of HC and PMO patients : osteoclasts differentiation was induced in PBMCs of HC and PMO patients with M-CSF (30 ng/ml) and RANKL (100 ng/ml) with or without SCFAs at 0.5 mM concentration for 14 days. Giant multinucleated cells were stained with TRAP and cells with > 3 nuclei were considered as mature osteoclasts. A) photomicrographs at different magnifications (10 X and 20X) were taken. (b-c) Number of TRAP positive cells with more than 3 nuclei in HC and PMO patients. Data is represented as mean \pm SEM. Mann-Whitney nonparametric test was performed for data analysis. Statistical significance was considered as $p \leq 0.05$ (* $p \leq 0.05$, ** $p \leq 0.01$, *** $p \leq 0.001$) with respect to indicated groups.

observations. Conclusively, our results pave way for targeted interventions via restoring the dysbiotic gut-microbial composition, thereby mitigating inflammatory bone loss observed under PMO conditions.

Discussion

Our group recently reported that numerical defect in the frequencies of Bregs and reduction in its tendency to produce IL-10 cytokine aggravate inflammatory bone loss in PMO.⁵ Several evidence suggest that gut microbial composition plays a crucial role in the development and

differentiation of host's immune system.^{1,8,20,21} Decisively, dysbiosis induced mucosal injury and leaky-gut are predominant contributors involved in the progression of pathological autoimmune disorders viz. RA, SLE etc.²² Emerging evidence suggest that GM possesses the ability to regulate the differentiation of Bregs and depletion of GM leads to reduction in the Bregs population and their tendency to produce IL-10.¹¹ Interestingly, in the present study, we observed that dysbiosis of GM contributes to inflammatory bone loss via modulating the "Bregs-Tregs-Th17" cell axis in PMO both under pre-clinical and clinical settings.

A study demonstrated that shortening of the colon length is employed as one of the biological markers for examining the inflammation of colon tissue.²³ In line with this, we too observed that colon length was significantly reduced in Ovx mice group in comparison to sham group, thereby suggesting toward the role of inflammation in gut under estrogen deficient conditions. In various inflammatory conditions, mucus layer of the intestine becomes more permeable to bacterial components and is linked with the severity of the disease.²⁴ In Crohn's disease, it has been observed that a marked increase in the intestinal permeability correlates with the severity of the disease.²⁵ A link between the systemic inflammation and impairment in the gut-integrity is further observed in RA patients and under sex steroid deficient conditions.^{11,26–28} To assess the gut-permeability/integrity under estrogen deficient post-menopausal conditions, we performed FITC-Dextran gut permeability assay. Notably, we found a significant enhancement in the gut-permeability/loss of gut-integrity in Ovx mice as demonstrated by the higher fluorescence of FITC-Dextran in the plasma of Ovx mice. In consistent to this, we too observed that the expression of tight junctional proteins such as claudin-1 and occludin were significantly reduced in the intestinal tissues of Ovx mice at transcriptomic level. In RA patients, it has been observed that the alpha diversity (richness and evenness) of microbial composition is significantly reduced and is further correlated with active RA.²⁹ Strikingly, we too observed that the alpha diversity was significantly reduced in the PMO patients, suggesting toward dysbiosis induced leaky gut in osteoporosis. A study reported that enhanced abundance of *Escherichia coli* along with a lower abundance of LAB producing bacteria such as *Lactobacillus*, *Bifidobacteria*, *Bacillus spp.* are reported to be linked with osteoporosis in IBD patients.^{30–32} Markedly, in RA patients *Bacteroides*, *Escherichia* and *Shigella* bacteria are found to be present in abundance whereas *Lactobacillus spp.* is observed to be lower in RA patients.^{17,33} In line with these observations, we too observed enhanced relative abundance of

Bacteroides and *Escherichia shigella* along with a lower abundance of LAB (i.e., *Lactobacillus spp.*) in osteoporotic patients. Thus, we next evaluated the potential of BC (LAB) in ameliorating the inflammatory bone loss in a pre-clinical mice model of osteoporosis. In 2009, Endres et al., assessed the safety of BC under *in vivo* conditions and reported that 9.52×10^{11} CFUs are safe and well tolerated for a 70 Kg human.¹⁵ Our study demonstrated that functionally compromised Bregs aggravate inflammatory bone loss in PMO. With an aim to investigate whether probiotics administration can restore the compromised anti-osteoclastogenic and immunomodulatory potential of Bregs even under Ovx condition, we employed BC in the present study. Interestingly, we observed that administration of BC conserved the microarchitecture of trabecular bone in Ovx mice. Notably, experimental outcomes evidently establish that BC has the potential to significantly enhance bone health via maintaining BMDs of femoral bone. Markedly, we observed that BC administration significantly enhanced the histomorphometric parameters viz. BV/TV% and Tb.Th along with significantly reducing Tb.Sp in Ovx mice. This data clearly suggests that BC exhibits anti-osteoporotic effect and maintains bone microarchitecture in Ovx mice. We further observed that supplementation of BC in Ovx mice significantly enhanced bone health via modulating the nexus between Bregs, Tregs, and Th17 immune cells. Of note, serum cytokine data further attested to the immunomodulatory potential of BC, where in administration of BC significantly reduced the levels of IL-17 cytokine (signature cytokine of osteoclastogenic Th17 cells) along with simultaneously enhancing IL-10 cytokine (signature cytokine of anti-osteoclastogenic Tregs and Bregs).

We next evaluated the potential of BC to restore the anti-osteoclastogenic potential of Bregs in Ovx mice. Interestingly, we observed that Ovx-Bregs have compromised anti-osteoclastogenic effect as compared to sham-Bregs. Remarkably, we observed that Bregs harvested from the Ovx + BC mice maintain the anti-osteoclastogenic effect, suggesting toward the

immunomodulatory potential of BC in ameliorating inflammatory bone loss in Ovx mice. Furthermore, we next explored whether along with maintaining the anti-osteoclastogenic potential of Bregs, can BC also improve the compromised immunomodulatory potential of Bregs in Ovx mice. For the same, Bregs isolated from either Sham/control mice, Ovx mice and Ovx + BC administered mice were co-cultured with naïve T cells. Flow cytometric data demonstrated that Sham-Bregs efficiently inhibited differentiation of Th17 cells while simultaneously inducing Tregsdifferentiation. On the contrary, Ovx-Bregs were unable to do so thereby reflecting the compromised functionality of Ovx-Bregs in comparison to Sham-Bregs. Enormously, we observed that BC administration maintains the immunosuppressive and immunomodulatory potential of Bregs, thereby suggesting toward the strong immunoporotic potential of BC even under estrogen-deficient conditions.

Moving ahead, we next asked the question whether BC administration modulates the functionality of Bregs via maintaining the gut integrity and restoring the dysbiotic-GM under estrogen deficient conditions. SCFAs have now taken the center stage as key players for their potential to positively affect the peripheral organs beyond the gut.³⁴ Of note, specialized bacteria belonging to the phyla Actinobacteria and Firmicutes are much more efficient in degradation of non-digestible polysaccharides (NDPs) and generating large quantities of SCFAs.³⁵ Our NGS data clearly represented reduction in the abundance of bacteria belonging to the phyla Firmicutes. This clearly suggests that reduction in abundance of Firmicutes is further linked with the SCFAs deprivation in osteoporotic mice model. Emerging evidence suggests that synthesis and production of SCFAs depends largely on the commensals that reside within the intestine e.g. acetate is produced by the phylum Bacteroidetes (largest group in intestine),³⁶ propionate by bacterial species (*Akkermansia muciniphila*)³⁵ and butyrate is being synthesized by four distinct pathways mainly glutamate, acetyl-CoA, lysine, and succinate.³⁷

Moving ahead, targeted metabolomic approach further attested that the concentration of SCFAs (acetate, propionate, and butyrate) was

significantly reduced in Ovx mice in comparison to the control group. A study reported that SCFAs via reducing the pH in the gut, contributes to the release of free calcium ions via decreasing the formation of calcium and phosphorus complexes,³⁸ thereby inducing the formation of bone under physiological condition. Several studies reported that SCFAs effectively suppress the onset of arthritis and lower the risk of RA.³⁹ Altogether, these studies suggest that reduction in the levels of SCFAs might augment inflammatory bone loss in PMO. Moreover, HPLC data further demonstrated that BC administration significantly enhanced the concentration of SCFAs in serum of Ovx mice. These results clearly suggest that BC via enhancing the levels of SCFAs ameliorate inflammatory bone loss in osteoporosis. Our *ex vivo* data demonstrated that all SCFAs (acetate, propionate, butyrate) significantly reduced the differentiation of multinucleated osteoclasts in a dose dependent manner. Nevertheless, among all the SCFAs, butyrate was the most potent and efficient anti-osteoclastogenic agent that inhibits osteoclastogenesis even at 0.125 mM. Flow cytometric data further revealed that all SCFAs were efficient in inducing the differentiation of Bregs. Tyagi et al., reported that butyrate producing bacteria via enhancing the frequencies of Tregs promote bone formation.²⁰ In the present study, we too observed that butyrate was the most potent SCFAs in enhancing not only the differentiation of Tregs, but also simultaneously inhibiting the differentiation of Th17 cells. Altogether, our data clearly establishes that among all the SCFAs, butyrate is the most potent anti-osteoclastogenic and immunomodulatory gut associated metabolite.

Furthermore, we next evaluated the anti-osteoporotic potential of butyrate in pre-clinical mice model of osteoporosis. In consistent to previous reported literature,³⁴ our micro-CT data clearly represented that the 3D microarchitecture of bones in Ovx mice administered with butyrate was significantly improved. Of note, it was further observed that butyrate administration significantly enhanced/restored the intestinal gut integrity under estrogen-deficient condition, along with significantly enhancing Tregs and Bregs and reducing Th17 cells at the prime site of osteoclastogenesis (i.e., bone marrow). Next, we were keen to know

whether these SCFAs do exhibit any anti-osteoclastogenic effect on human osteoclasts. Interestingly, in line with our pre-clinical study in Ovx mice, SCFAs do exhibit anti-osteoclastogenic effect even on human osteoclasts with significant reduction in the formation of multinucleated TRAP positive osteoclasts from human PBMCs. Moreover, SCFAs were further efficient in suppressing osteoclastogenesis in PBMCs of PMO patients. Altogether, among all the SCFAs, butyrate was found to be the most potent anti-osteoclastogenic agent in both murine and human studies.

Conclusively, the present study demonstrated the importance of dysregulated “Breg-Treg-Th17” cell axis in the pathophysiology of PMO and reveals the potential role of inflammatory milieu in augmenting bone loss in osteoporosis. Moreover, reduction in the alpha-diversity and relative-abundance of beneficial GM and lactic acid producing bacteria along with the enhancement in the endotoxin producing gram-negative bacteria in the gut further enhanced the inflammatory bone loss in PMO, thereby supporting our pre-clinical observations. Collectively, our experimental findings for the first time highlight the immunoporotic role of probiotic BC in skeletal homeostasis and emphasize its role as a novel immunoporotic agent in mitigating inflammatory bone loss even under PMO conditions via modulating the “Gut-Immune-Bone” axis.

Acknowledgment

LS, CS, and RKS acknowledge the Department of Biotechnology AIIMS, New Delhi-India for providing infra-structural facilities. LS thank ICMR ad-hoc project for research fellowship.

Disclosure statement

No potential conflict of interest was reported by the author(s).

Funding

This work was financially supported by the following projects: DBT[BT/PR41958/MED/97/524/2021], ICMR [61/05/2022-IMM/BMS] Govt. of India and AIIMS, Intramural project [AC-939] New Delhi-India sanctioned to RKS.

ORCID

Leena Sapra  <http://orcid.org/0000-0003-4558-580X>

Chaman Saini  <http://orcid.org/0000-0002-3609-6628>

Pradyumna K. Mishra  <http://orcid.org/0000-0002-0795-2819>

Bhavuk Garg  <http://orcid.org/0000-0003-3169-6437>

Rupesh K. Srivastava  <http://orcid.org/0000-0002-3323-0713>

Author contributions

RKS: conceptualization, methodology, validation, formal analysis, resources, writing original draft, visualization, supervision, project administration and funding acquisition. LS: Data curation, writing original draft, investigation, and formal analysis. CS: Data curation and formal analysis. PKM & SG: methodology and formal analysis. BG & VM: provided clinical samples and formal analysis.

Data availability statement

The data that support the findings of this study are available on request from the corresponding author.

Abbreviations

BC	<i>Bacillus coagulans</i>
SCFAs	Short Chain Fatty Acids
Bregs	Regulatory B cells
RANKL	Receptor activator of nuclear factor kappa B ligand
TLR	Toll like receptor
LPS	Lipopolysaccharide
IL	Interleukin
TGF	Transforming growth factor
RA	Rheumatoid arthritis
SLE	Systemic lupus erythematosus
PMA	Phorbol 12-myristate 13-acetate
BMCs	Bone marrow cells
M-CSF	Monocyte colony stimulating factor
TRAP	Tartrate resistant acid phosphatase
BMD	Bone mineral density
Tregs	Regulatory T cells
GM	Gut microbiota
PMO	Post-menopausal osteoporosis
μCT	Micro-computed tomography
HPLC	High-performance liquid chromatography
GALT	Gut associated lymphoid tissue
AhR	Aryl hydrocarbon receptor
GC	Germinal center
LAB	Lactic acid bacteria
FDA	Food and Drug Administration
GRAS	Generally recognized as safe
CFSE	Carboxyfluorescein succinimidyl ester
PP	Peyer's patches

References

1. Srivastava RK, Sapra L. The rising era of “Immunoporosis”: role of immune system in the pathophysiology of osteoporosis. *J Inflamm Res* [Internet]. 2022;15:1667–1698. <https://www.dovepress.com/the-rising-era-of-immunoporosis-role-of-immune-system-in-the-pathophys-peer-reviewed-fulltext-article-JIR>.
2. Srivastava RK, Dar HY, Mishra PK. Immunoporosis: immunology of osteoporosis—role of T cells. *Front Immunol* [Internet]. 2018;9. <http://journal.frontiersin.org/article/10.3389/fimmu.2018.00657/full>.
3. Woltman K, den Hoed PT. Osteoporosis in patients with a low-energy fracture: 3 years of screening in an osteoporosis outpatient clinic. *J Trauma Inj Infect Crit Care* [Internet]. 2010;69(1):169–173. <https://journals.lww.com/00005373-201007000-00026>.
4. Zhu X, Bai W, Zheng H. Twelve years of GWAS discoveries for osteoporosis and related traits: advances, challenges and applications. *Bone Res* [Internet]. 2021;9(1):23. doi: [10.1038/s41413-021-00143-3](https://doi.org/10.1038/s41413-021-00143-3).
5. Sapra L, Bhardwaj A, Mishra PK, Garg B, Verma B, Mishra GC, Srivastava RK. Regulatory B cells (Bregs) inhibit osteoclastogenesis and play a potential role in ameliorating ovariectomy-induced bone loss. *Front Immunol* [Internet]. 2021;12. <https://www.frontiersin.org/articles/10.3389/fimmu.2021.691081/full>.
6. Jiao Y, Wu L, Huntington ND, Zhang X. Crosstalk between gut microbiota and innate immunity and its implication in autoimmune diseases. *Front Immunol* [Internet]. 2020;11. <https://www.frontiersin.org/article/10.3389/fimmu.2020.00282/full>.
7. Ohlsson C, Sjögren K. Osteomicrobiology: a new cross-disciplinary research field. *Calcif Tissue Int*. 2018;102(4):426–432. doi: [10.1007/s00223-017-0336-6](https://doi.org/10.1007/s00223-017-0336-6).
8. Bhardwaj A, Sapra L, Tiwari A, Mishra PK, Sharma S, Srivastava RK. “Osteomicrobiology”: the nexus between bone and bugs. *Front Microbiol* [Internet]. 2022;12. <https://www.frontiersin.org/articles/10.3389/fmicb.2021.812466/full>.
9. Bhardwaj A, Sapra L, Madan D, Ahuja V, Sharma HP, Velpandian T, Mishra PK, Srivastava RK. Gut-resident Tregs (GTregs) play a pivotal role in maintaining bone health under post-menopausal osteoporotic conditions. *J Leukoc Biol* [Internet]. 2025; [10.1093/jleuko/qiaf008](https://doi.org/10.1093/jleuko/qiaf008).
10. Rosser EC, Oleinika K, Tonon S, Doyle R, Bosma A, Carter NA, Harris KA, Jones SA, Klein N, Mauri C. Regulatory B cells are induced by gut microbiota-driven interleukin-1 β and interleukin-6 production. *Nat Med* [Internet]. 2014;20(11):1334–1339. doi: [10.1038/nm.3680](https://doi.org/10.1038/nm.3680).
11. Rosser EC, Piper CJM, Matei DE, Blair PA, Rendeiro AF, Orford M, Alber DG, Krausgruber T, Catalan D, Klein N, et al. Microbiota-derived metabolites suppress arthritis by amplifying aryl-hydrocarbon receptor activation in regulatory B cells. *Cell Metab* [Internet]. 2020;31(4):837–851.e10. <https://linkinghub.elsevier.com/retrieve/pii/S1550413120301182>.
12. Pacaud M, Colas L, Brouard S. Microbiota and immunoregulation: a focus on regulatory B lymphocytes and transplantation. *Am J Transpl* [Internet]. 2021;21(7):2341–2347. <https://linkinghub.elsevier.com/retrieve/pii/S1600613522086233>.
13. Mishima Y, Oka A, Liu B, Herzog JW, Eun CS, Fan T-J, Bulik-Sullivan E, Carroll IM, Hansen JJ, Chen L, et al. Microbiota maintain colonic homeostasis by activating TLR2/MyD88/PI3K signaling in IL-10-producing regulatory B cells. *J Clin Invest* [Internet]. 2019;129(9):3702–3716. <https://www.jci.org/articles/view/93820>.
14. Chen Y, Wang X, Zhang C, Liu Z, Li C, Ren Z. Gut microbiota and bone diseases: a growing partnership. *Front Microbiol* [Internet]. 2022;13. <https://www.frontiersin.org/articles/10.3389/fmicb.2022.877776/full>.
15. Endres JR, Clewell A, Jade KA, Farber T, Hauswirth J, Schauss AG. Safety assessment of a proprietary preparation of a novel probiotic, *Bacillus coagulans*, as a food ingredient. *Food Chem Toxicol* [Internet]. 2009;47(6):1231–1238. <https://linkinghub.elsevier.com/retrieve/pii/S0278691509000933>.
16. Cao J, Yu Z, Liu W, Zhao J, Zhang H, Zhai Q, Chen W. Probiotic characteristics of *Bacillus coagulans* and associated implications for human health and diseases. *J Funct Foods* [Internet]. 2020;64:103643. <https://linkinghub.elsevier.com/retrieve/pii/S1756464619305675>.
17. Mandel DR, Eichas K, Holmes J. *Bacillus coagulans*: a viable adjunct therapy for relieving symptoms of rheumatoid arthritis according to a randomized, controlled trial. *BMC Complement Altern Med* [Internet]. 2010;10(1):1. [10.1186/1472-6882-10-1](https://doi.org/10.1186/1472-6882-10-1).
18. Vieco-Saiz N, Belguesmia Y, Raspoet R, Auclair E, Gancel F, Kempf I, Drider D. Benefits and inputs from lactic acid bacteria and their bacteriocins as alternatives to antibiotic growth promoters during food-animal production. *Front Microbiol* [Internet]. 2019;10. <https://www.frontiersin.org/article/10.3389/fmicb.2019.00057/full>.
19. Sapra L, Saini C, Mishra PK, Garg B, Gupta M, Srivastava RK. Compromised anti-osteoclastogenic and immunomodulatory functions of regulatory B cells (Bregs) aggravate inflammatory bone loss in post-menopausal osteoporosis. *Biochim Biophys Acta - Mol Basis Dis* [Internet]. 2025;1871(3):167675. <https://linkinghub.elsevier.com/retrieve/pii/S0925443925000201>.
20. Tyagi AM, Yu M, Darby TM, Vaccaro C, Li J-Y, Owens JA, Hsu E, Adams J, Weitzmann MN, Jones RM, et al. The microbial metabolite butyrate stimulates bone formation via T regulatory cell-mediated regulation of WNT10B expression. *Immunity* [Internet]. 2018;49(6):1116–1131.e7. doi: [10.1016/j.immuni.2018.10.013](https://doi.org/10.1016/j.immuni.2018.10.013).
21. Sapra L, Saini C, Garg B, Gupta R, Verma B, Mishra PK. Long - term implications of COVID - 19 on bone

- health: pathophysiology and therapeutics. *Inflamm Res* [Internet]. 2022; 71(9):1025–1040. doi: [10.1007/s00011-022-01616-9](https://doi.org/10.1007/s00011-022-01616-9).
22. Kinashi Y, Hase K. Partners in leaky gut syndrome: intestinal dysbiosis and autoimmunity. *Front Immunol* [Internet]. 2021;12. <https://www.frontiersin.org/articles/10.3389/fimmu.2021.673708/full>.
 23. Jin B-R, Chung K-S, Cheon S-Y, Lee M, Hwang S, Noh Hwang S, Rhee K-J, An H-J. Rosmarinic acid suppresses colonic inflammation in dextran sulphate sodium (DSS)-induced mice via dual inhibition of NF- κ B and STAT3 activation. *Sci Rep* [Internet]. 2017;7(1):46252. <https://www.nature.com/articles/srep46252>.
 24. Bischoff SC, Barbara G, Buurman W, Ockhuizen T, Schulzke J-D, Serino M, Tilg H, Watson A, Wells JM. Intestinal permeability – a new target for disease prevention and therapy. *BMC Gastroenterol* [Internet]. 2014;14(1):189. [10.1186/s12876-014-0189-7](https://doi.org/10.1186/s12876-014-0189-7).
 25. Hollander D. Increased intestinal permeability in patients with crohn's disease and their relatives. *Ann Intern Med* [Internet]. 1986;105:883. <http://annals.org/article.aspx?doi=10.7326/0003-4819-105-6-883>.
 26. Li J-Y, Chassaing B, Tyagi AM, Vaccaro C, Luo T, Adams J, Darby TM, Weitzmann MN, Mulle JG, Gewirtz AT, et al. Sex steroid deficiency-associated bone loss is microbiota dependent and prevented by probiotics. *J Clin Invest* [Internet]. 2016;126(6):2049–2063. <https://www.jci.org/articles/view/86062>.
 27. Tyagi AM, Darby TM, Hsu E, Yu M, Pal S, Dar H, Li J-Y, Adams J, Jones RM, Pacifici R. The gut microbiota is a transmissible determinant of skeletal maturation. *Elife* [Internet]. 2021;10. <https://elifesciences.org/articles/64237>.
 28. Li J-Y, Yu M, Pal S, Tyagi AM, Dar H, Adams J, Weitzmann MN, Jones RM, Pacifici R. Parathyroid hormone-dependent bone formation requires butyrate production by intestinal microbiota. *J Clin Invest* [Internet]. 2020;130(4):1767–1781. <https://www.jci.org/articles/view/133473>.
 29. Jeong Y, Kim J-W, You HJ, Park S-J, Lee J, Ju JH, Park MS, Jin H, Cho M-L, Kwon B, et al. Gut microbial composition and function are altered in patients with early rheumatoid arthritis. *J Clin Med* [Internet]. 2019;8:693. [10.3390/jcm8050693](https://doi.org/10.3390/jcm8050693).
 30. Liu Q, Mak JWY, Su Q, Yeoh YK, Lui G-Y, Ng SSS, Zhang F, Li AYL, Lu W, Hui D-C, et al. Gut microbiota dynamics in a prospective cohort of patients with post-acute COVID-19 syndrome. *Gut* [Internet]. 2022;71(3):544–552. [10.1136/gutjnl-2021-325989](https://doi.org/10.1136/gutjnl-2021-325989).
 31. Liu Y, Yin F, Huang L, Teng H, Shen T, Qin H. Long-term and continuous administration of *Bacillus subtilis* during remission effectively maintains the remission of inflammatory bowel disease by protecting intestinal integrity, regulating epithelial proliferation, and reshaping microbial structure and function. *Food Funct* [Internet]. 2021;12(5):2201–2210. <https://xlink.rsc.org/?DOI=D0FO02786C>.
 32. Takimoto T, Hatanaka M, Hoshino T, Takara T, Tanaka K, Shimizu A, Morita H, Nakamura T. Effect of *Bacillus subtilis* C-3102 on bone mineral density in healthy postmenopausal Japanese women: a randomized, placebo-controlled, double-blind clinical trial. *Biosci Microbiota, Food Heal* [Internet]. 2018;37(4):87–96. https://www.jstage.jst.go.jp/article/bmfh/37/4/37_18-006/_article.
 33. Wells PM, Adebayo AS, Bowyer RCE, Freidin MB, Finckh A, Strowig T, Lesker TR, Alpizar-Rodriguez D, Gilbert B, Kirkham B, et al. Associations between gut microbiota and genetic risk for rheumatoid arthritis in the absence of disease: a cross-sectional study. *Lancet Rheumatol* [Internet]. 2020;2(7):e418–27. <https://linkinghub.elsevier.com/retrieve/pii/S2665991320300643>.
 34. Lucas S, Omata Y, Hofmann J, Böttcher M, Iljazovic A, Sarter K, Albrecht O, Schulz O, Krishnacoumar B, Krönke G, et al. Short-chain fatty acids regulate systemic bone mass and protect from pathological bone loss. *Nat Commun* [Internet]. 2018;9(1):55. doi: [10.1038/s41467-017-02490-4](https://doi.org/10.1038/s41467-017-02490-4).
 35. van der Hee B, Wells JM. Microbial regulation of host physiology by short-chain fatty acids. *Trends Microbiol* [Internet]. 2021;29(8):700–712. <https://linkinghub.elsevier.com/retrieve/pii/S0966842X21000354>.
 36. Cummings JH, Pomare EW, Branch WJ, Naylor CP, Macfarlane GT. Short chain fatty acids in human large intestine, portal, hepatic and venous blood. *Gut* [Internet]. 1987;28(10):1221–1227. doi: [10.1136/gut.28.10.1221](https://doi.org/10.1136/gut.28.10.1221).
 37. Louis P, Flint HJ. Formation of propionate and butyrate by the human colonic microbiota. *Environ Microbiol* [Internet]. 2017;19(1):29–41. doi: [10.1111/1462-2920.13589](https://doi.org/10.1111/1462-2920.13589).
 38. Han D, Wang W, Gong J, Ma Y, Li Y. Microbiota metabolites in bone: shaping health and confronting disease. *Heliyon* [Internet]. 2024;10(7):e28435. doi: [10.1016/j.heliyon.2024.e28435](https://doi.org/10.1016/j.heliyon.2024.e28435).
 39. Martinsson K, Dürholz K, Schett G, Zaiss MM, Kastbom A. Higher serum levels of short-chain fatty acids are associated with non-progression to arthritis in individuals at increased risk of RA. *Ann Rheum Dis* [Internet]. 2022;81(3):445–447. [10.1136/annrheumdis-2021-221386](https://doi.org/10.1136/annrheumdis-2021-221386).